

**INTEGRATED 3D SEISMIC MODELLING OF
LOWER GORU SANDS IN GAMBAT LATIF BLOCKS IN
PAKISTAN BASED ON STRUCTURAL
INTERPRETATION, SEQUENCE STRATIGRAPHY,
SEISMIC ATTRIBUTES AND FACIES ANALYSES.**



By

LAIQUE ZADA S/O LAL ZADA

(02112111005)

M.PHIL. (Geophysics)

2021-2023.

DEPARTMENT OF EARTH SCIENCES

QUAID-I-AZAM UNIVERSITY

ISLAMABAD

CERTIFICATE OF APPROVAL

This dissertation submitted by **LAIQUE ZADA S/O LAL ZADA** is accepted in its present form by the Department of Earth Sciences, Quaid-I-Azam University Islamabad as satisfying the requirement for the award of degree of M.Phil. Geophysics.

RECOMMENDED BY

Prof. Dr. Monalisa (Supervisor)

Dr. Aamir Ali (Chairman)

Dr. Shahid Nadeem Qureshi

External Examiner

ACKNOWLEDGEMENT

In the name of the Most Generous and Most Merciful Allah. All thanks are due to the all-powerful Allah, the universe's creator. Second, I want to express my sincerest gratitude to the Prophet Muhammad (Peace Be Upon Him). I would not be able to finish my work or be in such a place without Allah's grace. Thanks to the help and direction of many people, this thesis is now available in its current form. I would like to take this opportunity to thank everyone who helped me and contributed to the completion of this thesis.

I would like to convey my sincere gratitude to **Professor Dr. MONALISA** for giving me the chance to work with her on such a great study. This thesis is feasible because of her unwavering encouragement, and support. I appreciate her taking responsibility for my errors and serving as the "teacher" for those who don't grasp the significance of the exalted position conferred upon them.

Additionally, I'm delighted to officially express my sincere gratitude and appreciation to **Mr. Zahid Ullah Khan**, my senior Yawar Amin, and Dr. Muhammad Tayyab Naseer, my friends, Chaudhary Umar Ghaffar, Ahmed Rafeh, Aftab Shabeer and a host of others without the aid of whom I could not have successfully accomplished this course assignment.

I would also like to convey my Gratitude to OGDCL and the Officers who helped me and guide me during my CSR One-year paid internship to work on the Software's.

Finally, I want to thank my family for their unwavering encouragement, persistent prayers, and well wishes. My parents deserve the most gratitude for their unwavering support throughout the years and for making it possible for me to successfully complete my thesis. Those who were left out of the acknowledgment are always dear to my heart, and they are fully appreciated even if they aren't mentioned.

LAIQUE ZADA
M.Phil. GEOPHYSICS
2021-2023

Contents

List of Figures.....	7
List of Tables.....	10
CHAPTER 01.....	13
INTRODUCTION.....	13
1.1 Introduction.....	13
1.2 Objectives.....	14
1.3 Study Area.....	14
1.4 Methodology.....	15
CHAPTER 02.....	18
GEOLOGY OF STUDY AREA.....	18
2.1 Introduction.....	18
2.2 Structural Setting of Study Area.....	18
2.3 Tectonics Setting.....	19
2.4 Stratigraphy of the Study Area.....	19
2.5 Petroleum Play of Study Area.....	22
2.5.1 Source Rock.....	22
2.5.2 Reservoir Rock.....	22
2.5.3 Seal Rock.....	22
CHAPTER 03.....	23
3D SEISMIC DATA INTERPRETATION.....	23
3.1 Introduction.....	23
3.2 Base Map.....	23
3.3 Seismic to Well Tie.....	23
3.4 Faults Correlation and Fault Polygon Generation.....	25
3.5 Horizon Identification.....	25
3.6 Contour Map Preparation.....	26
3.7 Time Contour Map Interpretation.....	27
3.8 Depth Contour Map Interpretation.....	27
3.9 Seismic Attributes Analysis.....	33
3.9.1: Pre-Stack Attributes.....	34
3.9.2: Post Stack Attributes.....	34
3.9.3: Physical Attributes.....	34

3.9.4: Geometrical attributes	34
3.9.5: Instantaneous-Dip Attribute	35
3.9.6: Shale Indicator.....	35
CHAPTER 04	37
PETROPHYSICAL ANALYSIS	37
4.1 Introduction	37
4.2 Reservoir Petrophysical Properties.....	37
4.2.1 Lithology.....	37
4.2.2 Porosity (ϕ)	37
4.2.3 Water Saturation (S_w).....	37
4.2.4 Hydrocarbon Saturation (S_h)	38
4.2.5 Net Pay	38
4.3 Classification of Geophysical Well Logs	38
4.3.1 Lithology Logs.....	38
4.3.2 Resistivity Logs	39
4.3.3 Porosity Logs	40
4.4 Average Porosity (ϕ_{avg})	41
4.5 Effective Porosity (ϕ_e)	42
4.6 Water Saturation (S_w).....	42
4.7 Hydrocarbon Saturation (S_h).....	45
4.8 Interpretation of Well Logs	45
CHAPTER 05	49
Seismic Inversion Analysis.....	49
5.1 Introduction.....	49
5.2 Wavelet Extraction	49
5.3 Well-to-Seismic Tie.....	50
5.4 Initial Model/Low Frequency (LF) Model	51
5.5 Model-Based Inversion.....	52
5.3 Lambda-Mu-Rho Inverted Properties.	55
Chapter 6	60
Electrofacies and Sequence Stratigraphy.....	60
6.1 Introduction.....	60
6.2 Methodology	60
6.3 Electrofacies Classification	61

6.4 Fuzzy Classification Method	62
6.5 Tool for facies interpretation:	63
6.5.1 Cylindrical shape:	64
6.5.2 Funnel Shape:	64
6.5.3 Bell shape:	64
6.5.4 Bow shape:	64
6.5.5 Irregular shape:	64
6.6 Results and Discussion	65
6.7 Zone of Interest	67
6.8. Introduction to sequence stratigraphy:	68
6.8.1. Methodology	70
6.8.1.1. Wireline Logs Sequence Stratigraphy:	70
6.8.2. Description of Sequences based on GR log	72
CHAPTER 07	76
DISCUSSIONS AND CONCLUSIONS.....	76
7.1 Discussions	76
References.....	79

DRSML QAU

List of Figures

- Figure 1.1 Generalized map of the study area, with block boundaries of the Gambat-Latif block highlighted in Lower Indus Basin (Kazmi and Rana, 1982)15.
- Figure 1.2: The workflow followed in this study.....17.
- Figure 2.1 Tectonic and sedimentary basin of Pakistan (modified from Aziz & Khan, 2003), with the study area defined within the highlighted black box.20.
- Figure 2.2 Schematic stratigraphic char of the Lower Indus Basin, with the reservoir interval under study (C sand) part of the Lower Goru formation (modified from Abbasi et al.,2016)21.
- Figure 3.1 Spatial coverage of the seismic and well log data utilized in the study, with the base map constructed on IHS Kingdom software, based on Universal Transverse Mercator 42N coordinate system.24.
- Figure 3.2 synthetic seismogram generated using the sonic and density logs from Tajjal-03 las file, for the seismic to well tie between well log and seismic data. Horizons have been marked based upon this tie.....25.
- Figure 3.3 Inline 1336 with well displayed overlain by the trace obtained from seismic to well tie, marking the horizons as identified by synthetic seismogram on IHS Kingdom software.26.
- Figure 3.4 Time contour map of B Sands with a contour interval of 0.01s, spatially distributed on the base map with a maximum of 2.290s and minimum of 2.220s, created on IHS Kingdom software.....28.
- Figure 3.5 Time contour map of C Sands with a contour interval of 0.01s, spatially distributed on the base map with a maximum of 2.23s and minimum of 2.17s, created on IHS Kingdom software.29.
- Figure 3.6 Time contour map of D Sands with a contour interval of 0.01s, spatially distributed on the base map with a maximum of 2.24s and minimum of 2.16s, created on IHS Kingdom software.....30.

Figure 3.7 Depth contour map of B Sands with a contour interval of 20m, spatially distributed on the base map with a maximum of 3660m and minimum of 3560m, created on IHS Kingdom software.	31.
Figure 3.8 Depth contour map of C Sands with a contour interval of 16m, spatially distributed on the base map with a maximum of 3496m and minimum of 3476m, created on IHS Kingdom software.	32.
Figure 3.9 Depth contour map of D Sands with a contour interval of 16m, spatially distributed on the base map with a maximum of 3440m and minimum of 3360m, created on IHS Kingdom software.	33.
Figure 3.10: Time slice of Instantaneous dip attribute at 2.3 seconds.....	35.
Figure 3.11: Time slice extracted for shale indicator at 2.4 seconds.....	36.
Figure 4.1 Determination of Rweq from SP-1 chart uses the well data header file to find resistivity of water equivalent of water (Schlumberger,1989)	44.
Figure 4.2 Determination of Rw from SP-3 chart after determining Rweq and using formation temperature curves can be utilized to determine where Rw for given well fits best (Schlumberger, 1989)	45.
Figure 4.3 Interpreted section of Tajjal-02 well in the C Sands, where possible C sands presence can be confirmed with low volume of shale and high porosity, with two zones of interest identified with zone 1 having a net pay of 14m, while zone 2 having 7m...48.	
Figure 5.1. The statistical wavelet extracted from the seismic data with a wavelength of 0.02s.....	50.
Figure 5.2. The correlation shows adequate matching of the extracted wavelet with recorded seismic data, hence making it suitable for inversion.....	51.
Figure 5.3: Cross section view of inline 1346 displaying the initial acoustic impedance values based on logs of Tajjal-03 created using Hampson and Russell (HRS) software.....	52.

Figure 5.4: Statistical wavelet convolved with the extracted low frequency induced calculated geological model of the area for minimizing the uncertainty between calculated and observed models, with a 99% correlation was achieved using Hampson and Russel (HRS).....53.

Figure 5.5: Cross section view of inline 1346 displaying the acoustic impedance contrast of lithologies with low impedance as sands, created using Hampson and Russell (HRS) software.....54.

Figure 5.6: Acoustic impedance based on Model based inversion indicating potential prospect zone where the impedance values are relatively low.....55.

Figure 5.7 Spatial distribution of the acoustic impedance utilizing lambda-rho attributes, indicating similar pattern to model-based inversion spatial distribution but more refined to gas saturated reservoir sands, created using Hampson and Russell (HRS).....56.

Figure 5.8: Lambda-rho attribute of the zone of interest in C-Interval indicating a potential prospect zone where the lambda-rho values are low, created using Hampson and Russel.....57.

Figure 5.9: Mu-rho attribute applied to Tajjal-03 well, an attribute much sensitive to rock matrix indicates low acoustic impedance highlighted with green to yellow color as reservoir sand being porous sand bodies, created using Hampson and Russell (HRS).....58.

Figure 5.10: Mu-rho attribute slice of the zone of interest indicating that the identified potential prospect zone has moderate Mu-rho values. Using Hampson and Russel Software.....59.

Figure 6.1 Flowchart showing the steps of electrofacies classification.....60.

Figure 6.2- Facies correlation with a variety of other log shapes regarding the sedimentological relationship (Nazeer et al., 2016; Selley, 1979)65

Figure 6.3: IPSOM electrofacies classification and self-organizing maps of Tajjal-02 based on Gamma ray (Dark grey color), Resistivity (Blue color), Thermal Neutron Porosity (Orange color), Bulk density (Brown color), and Sonic logs (Red color)66.

Figure.6.4: The electrofacies of well Tajjal-02 indicating four lithologies namely, shale (blue color), shaly sand (sky blue color), gas sand (cyan color), sandy shale (green color)67.

Figure. 6.5. Shapes of GR logs (bell, cylindrical & funnel) show different lithology to bell shapeslog (Serra & Sulpice, 1975; Rider, 1986).....70.

Figure. 6.6. A funnel shape geometry of the log (left) coursing upward sequence and grain size GR correlation (Rider, 1986)71.

Fig. 6.7. Another example of GR log that are showing point bars, channels, progradational, aggregational and transgressive facies environment and grain sizes of various facies (Serra, 1972; Parker, 1977; Galloway and Hobday, 1983.....72.

Figure.6.8(a): Correlation of sequence in wells.....73.

Figure.6.8(b): Correlation of sequence in wells.....74.

List of Tables

Table 4.1 Results determined for petrophysical analysis of Tajjal-02 well with two zones of interest identified, with their calculate attributes of porosity, water saturation, and hydrocarbon saturation being the following.....47.

Table.6.1: The reservoir potential zones shown in the table below.....67.

ABSTRACT

Reservoir properties are essential for quantitative and qualitative reservoir evaluation. Although the interpretation of seismic data and petrophysical analysis of well logs provides a crude analysis of the reservoir, the spatial distribution of reservoir characteristics is essential for economical exploitation. The objective of this study is to characterize the spatially distributed reservoir properties of Lower Goru sands over a vintage 3D seismic data in Gambat-Latif block, Lower Indus Basin, Pakistan, using structural interpretation, attribute analysis, inversion, and Lambda-Mu-Rho (LMR) attributes. C Sands has been identified using well to seismic tie, with horizons picked on the 3D seismic data. Interpreted seismic volume shows presence of faults in subsurface, with faults oriented in a NW-SE direction, and marked horizons of interest as shallow in west and deeper in the east, with deposition of facies also showing a thickening trend towards east. Petrophysical analysis conducted in both the wells, out of which two zones of interest were marked in Tajjal-02 well showing an average high effective porosity in Zone-1 ranging from 11-12 %, and in Zone-2 ranging from 7-8 % and water saturation in Zone-1 ranging from 74.97-75 %, and in Zone-2 ranging from 80-81 %.

The inverted acoustic impedance volume identified the gas sand lithology and confirmed the presence of fluid in the C sands using model-based inversion and lambda-mu-rho attribute. The picked horizons have been used to mark the spatial distribution of the quantitative reservoir properties. Model based inversion depicts low acoustic impedance anomalous zones in the sands of C Sands indicating the presence of hydrocarbons. The mu-rho attribute spatially indicates low to moderate values confirming the presence of sands, while the lambda-rho attribute, sensitive to pore fluids, confirms the presence of oil saturated sands of C Sands.

A new location has been proposed for drilling well where there is a potential prospect zone based on the analysis. The proposed location has low impedance values, low to moderate Mu-Rho values and low Lambda-rho values all supporting the presence of hydrocarbon accumulation.

The Electrofacies have been generated from the well log data indicating four facies namely, gas sand, shaly sand, sandy shale, and shale. Gas sands are observed in the well with the help of electro facies. Sequence stratigraphy is applied on well data and sequences are marked with the help of well logs. The result indicates a zone in Tajjal -03, two Zones in well Tajjal-02 and two zones in well South Tajjal-01

DRSML QAU

CHAPTER 01

INTRODUCTION

1.1 Introduction

Pakistan is a country with abundant mineral resources, yet many industries and day to day life runs on technology powered by hydrocarbons, which is a commodity that the country still lacks. The exploration of hydrocarbons is carried out by the industry using conventional methods; however, the exploitation of reservoirs can only be enhanced by properly characterizing the reservoirs. The estimation of key physical parameters including porosity, permeability, lower and upper reservoir limits, their lateral and vertical extent, heterogeneous nature, and the volume and type of subsurface fluids are all part of reservoir characterization (Bacon et al., 2007; Avseth et al., 2005). The data typically utilized for estimation of the reservoir properties are seismic and well log data, however Drill Stem Test (DST) and core cuttings of the wells help in constraining the data to limit uncertainties in the study. These data sets can be combined to study and estimate reservoir properties at different scales (Hearts et al., 2002; Chen and Sidney, 1997; Chopra and Marfurt, 2007; King, 1990; Lindseth, 1979). To efficiently link the data sets different interpolation or other geostatistical techniques are utilized to enhance the data to observations made in field and create a tie with the local geology (Bosch et al., 2010).

There is an understanding that even the most calibrated data set can still have erroneous recordings, hence, hindering the actual outcomes of the parameters calculated for reservoir characterization. An understanding of quality check is therefore kept on the data sets, especially the well log data set, in which certain templates can be utilized to further validate the well log data sets in the absence of core cuttings. This helps in reducing the degree of uncertainty while characterizing the reservoir rock.

Although qualitative analysis utilizes the interpretation of tracking horizons in context to the geologic structures in subsurface, following the stratigraphic normal sequence, the true goal for any geoscientist in the upstream sector lies in the mapping of zones of hydrocarbon accumulations. Seismic reflectors can be mapped spatially through travel time, but the quantitative characteristics pertaining to the reservoir are somewhat still an ambiguity.

Seismic and well log data, coupled with inversion of the seismic volume set can be integrated to stem reservoir parameters (Landa et al., 2000; Simm & Bacon, 2014). The refined logs from the well can further be utilized in seismic inversion techniques to retrieve acoustic impedance from the seismic data, giving key insight to the distinctive reservoir parameters, spatial distribution of the deposition, and local petrophysical properties (Bosch et al., 2009; Angeleri and Capri, 1982; Walls et al., 2004; Yao and Gan, 2000; Grana and Dvorkin, 2011). An important aspect of seismic inversion is its ability to enhance the vertical resolution of the data (Delaplanche et al., 1982), therefore improving our interpretation, because layer-oriented impedance displays are more helpful in constraining the reservoir models (Ashcroft, 2011). The data set used in this study is post-stack seismic 3D data and well log data of Tajjal-02,03. The inversion techniques applied to the data set includes model-based inversion (for acoustic and shear impedance) and lambda rho-mu rho (LMR) attribute, each working on a different set of algorithms (Veeken 2007; Silva et al., 2004; Veeken and Silva et al., 2004; Ashcroft, 2011; Veeken and Davies, 2006; Wang, 2017).

1.2 Objectives

- Structural interpretation of the study area and demarcation of the horizon of interest using time and depth contours.
- Petrophysical analysis of the Tajjal-02 to mark the favorable zones of hydrocarbon and understand the reservoir properties of C sands.
- Characterization of C sand reservoir potential using post-stack model-based inversion with the help of logs using well Tajjal-03.
- Developing lambda-rho and mu-rho attributes from the acoustic and shear impedance volumes for determining the presence of fluid and confirmation of sand lithology in the reservoir respectively.
- Determining Facies and sequence of the area through electrofacies and sequence stratigraphy by using the well log data.

1.3 Study Area

The area of study is in the Khairpur district of Sindh in the Lower Indus Basin of Pakistan, lying on the eastern flank of Khairpur high. Khairpur high has a high geothermal gradient suffering through many stages of subsidence. It is situated at 27° 21' N and 68° 31' E having an average altitude of 47m. The block being operated by

OMV is situated almost 120km southeast of Sukkur with the size of 3D project covered of 675 square kilometers wherein 11 square kilometers was approved for the purpose of dissertation, with the study area shown below in Figure 1.1.

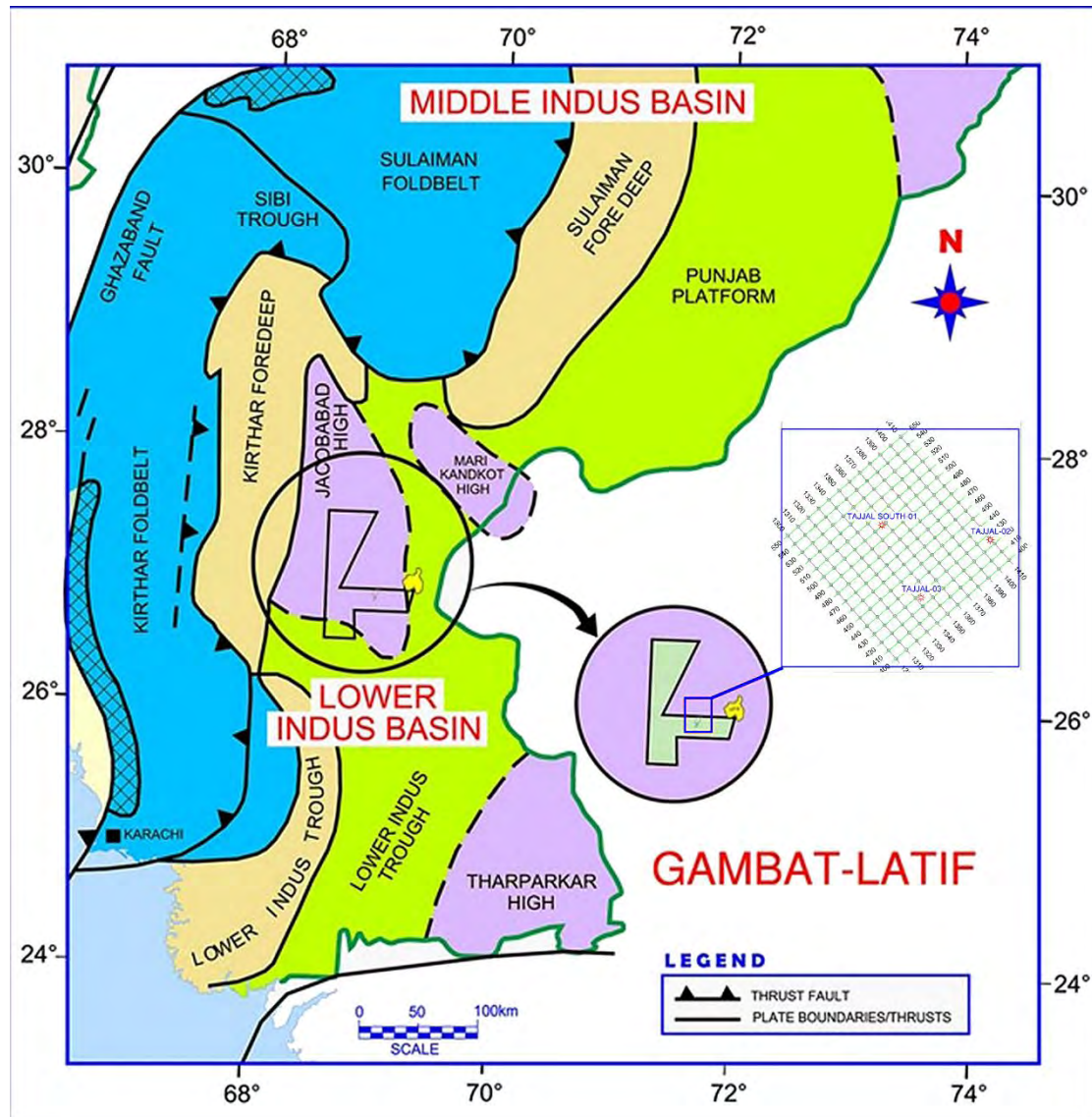


Figure 1.1: Generalized map of the study area, with block boundaries of the Gambat-Latif block highlighted in Lower Indus Basin (Kazmi and Rana, 1982).

1.4 Methodology

Synthetic seismogram is generated at the well location of Tajjal-03 with the help of well logs data to identify various horizons of interest and correlate well and seismic data. To get the best correlation between well and seismic data, well-seismic tie operation was performed. Various faults and horizons of interest at reservoir level have been interpreted in the given seismic cube. For regional propagation and extension of

fault plane marked on various seismic In-lines, faults polygons and grids have been generated for contouring to interpolate the marked horizons on the whole seismic cube.

Petrophysical analysis was performed to evaluate reservoir pores volume, shale volume, water, and presence of economical quantity of hydrocarbon saturation in sand reservoir. Seismic attribute analysis has been carried out on the seismic data. Two attributes have been applied which are instantaneous dip attribute and shale indicator attribute.

Facies analysis has been done on the well data. Electro facies have been calculated for the better understanding of the reservoir. Sequence stratigraphy has also been applied to the well data to determine the sequences in the study area. Different depositional patterns have been identified on the log data with help of different lithological logs.

Finally, the post stack model-based inversion has been applied for impedance spatial distribution. By using the inverted P-impedance and S-impedance volumes, lambda-mu-rho (LMR) attributes have been generated. These properties have been utilized to identify the spatial distribution of the sands and in turn characterize the reservoir. The whole workflow has been shown in the Figure1.2 below:

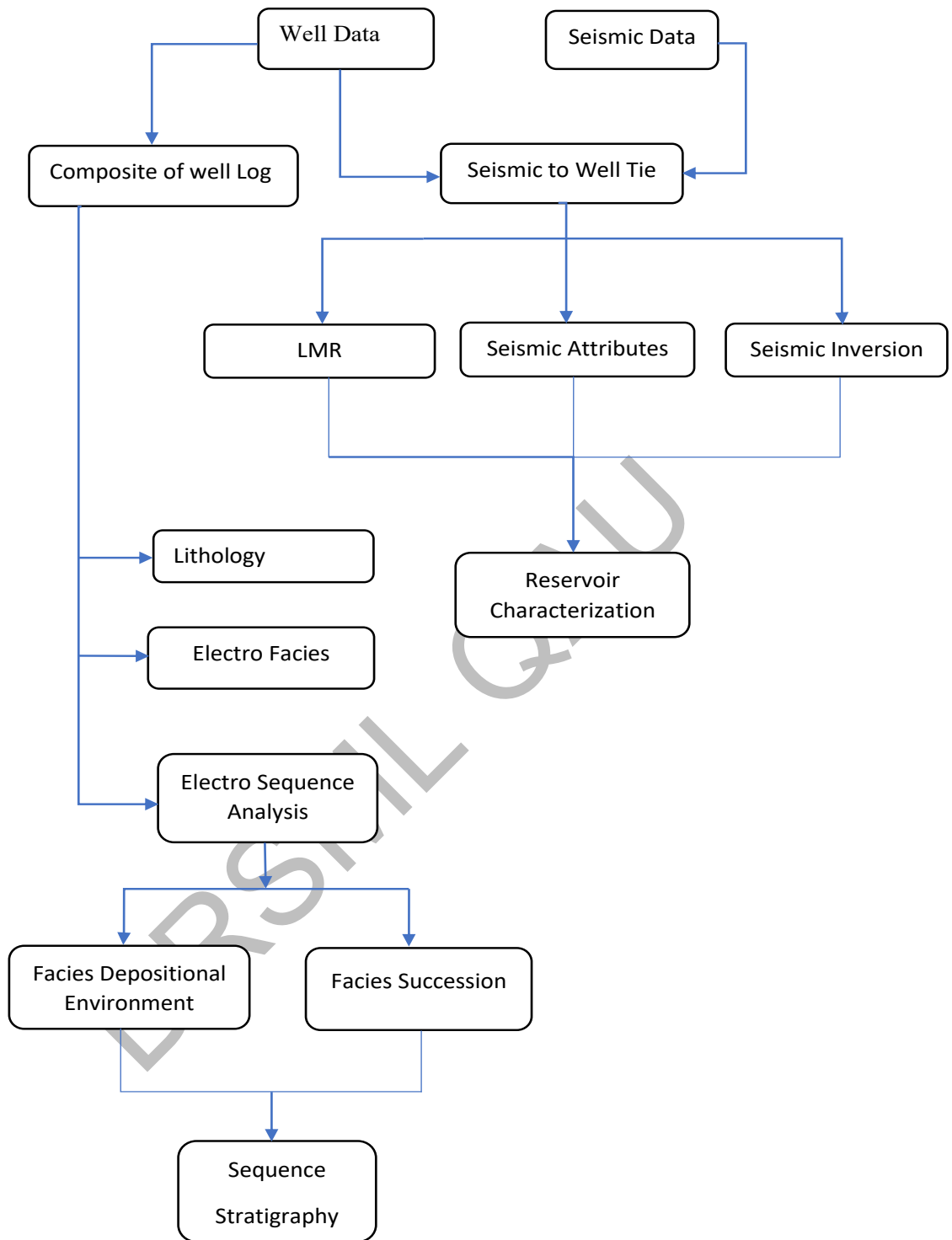


Figure 1.2: The workflow followed in this study.

CHAPTER 02

GEOLOGY OF STUDY AREA

2.1 Introduction

The tectonic settings, geology, and sequence stratigraphy of the research area are the most crucial inputs for the search of hydrocarbons. The tectonic and depositional sequences of the basin can be pieced together using the evolution of the basin (Kingston et al., 1983). For geoscientists to successfully plan and carry out geophysical research in each location, they must have a solid understanding of its geology and structural characteristics. An interpreter should have a firm understanding of the region's geology, the strata of the lithologies, unconformities, and key structures of the study area to manage such elaborate and complex plans while taking into consideration time and resources (Kazmi & Jan, 1997). In this chapter, the structural geology, stratigraphy, and tectonic settings of the region are briefly described.

2.2 Structural Setting of Study Area

According to the discussion above, the Lower Indus Basin, Pakistan's geological province, is in the northwest of Sindh, which is where the research region for the block Gambat-Latif is located. The area is classified as an extensional regime area, and faults are found where there is a break in the lithologies or bedding. These extensional regimes are characterized by normal faults, which are typically linked with horst and graben formations (Kadri, 1995).

The block, known as the Kirthar Foredeep, is on the Indian Craton's continental shelf and is located southeast of the Kirthar fold and thrust belt. Since the Lower Indus Basin is essentially a cratonic marginal basin that edges the Indian Shield to the northwest, it has a high potential for numerous exploratory plays and traps that are structural, stratigraphic, or a mix of the two. A highly mature field can be distinguished from neighboring producing blocks by its mature source rock and hydrocarbon ejection, a good reservoir rock with a suitable dip and fault-bounded trap, stratigraphic lenses in some areas, and the presence of both lateral and vertical sealing rocks to preserve the integrity of the petroleum system. The Lower Goru sands from the Cretaceous are the area's main reservoir rocks, and they are unconformably overlain by Paleocene Deccan Basaltic eruptions and Tertiary sedimentation (Shah et al., 1977).

2.3 Tectonics Setting

The Sukkur Rift Zone, a collective term for the Jacobabad-Mari Highs with an aerial extension spanning from the Baluchistan basin in the west to the Indian shield in the east, is where the Lower Indus Basin begins (Raza et al., 1989). The Main frontal thrust bounds the Kirthar fold and thrust belt in the east running along the western margin of River Indus. West of Kirthar fold and thrust belt adjoins the Chagai Magmatic Arc System and Pishin basin, with its boundary demarcated by suture zones of Bela and Muslim Bagh, having developed along strike slip components of the Chaman Fault and Ornach-Nal Fault. Kirthar foredeep initiates from the eastern margin of the fold belt and extends eastwards to Thar Platform, which is characterized by gentle sloping monocline, extending towards the exposed Indian craton as the Nagar Parker igneous complex in the east, merging in the Kirthar trough in southwest, and bounded by Sulaiman Fold belt in the northwest (Shah,2009). The generalized tectonic map with structural settings is displayed below in Figure 2.1.

2.4 Stratigraphy of the Study Area.

Gambat block is covered mainly by the alluvium deposited by river Indus, with sedimentation cover being recorded throughout the geological time in the area under study. The stratigraphy of the Lower Indus basin is mostly associated to the Indian cratons rifting and drifting through the Tethyan ocean. Rifting and subsequent Kimmeridgian-Oxfordian unconformity a set development of bathyal and pelagic shales on Jurassic Chiltan limestone of the platform area can be seen with an onset of transgression with a resultant of Sembar formation with a shallow marine depositional environment is observed.

This event was subsequently followed by sea level changes and tectonics during the time which resulted in prograding siliciclastic wedges of Sembar and Goru formations. The relative change of sea level after Sembar formation deposition, continued to change, at first causing an overall retrogradation of basin margin, through which sand bearing facies of various environments that included deltaic, shoreface and barrier islands started depositing in the form of Lower Goru of Cretaceous. However, the style changed from retrogradation to prograding, with shale deposition sequence starting to deposit namely as Upper Goru of Early Cretaceous (Raza et al., 1989).

The important unconformities marked around study are at base of Pleocene and Plio-Miocene. Sedimentary succession comprising of Nari of Oligocene and Gaj formation of Miocene is not encountered in most of the wells, that could have been eroded or never deposited due to uplifting in Late Tertiary. Tectonic and sedimentary basin of Pakistan with the study area defined within the highlighted black box as shown in figure 2.1 The stratigraphy chart for Lower Indus basin can be seen below in Figure 2.2.

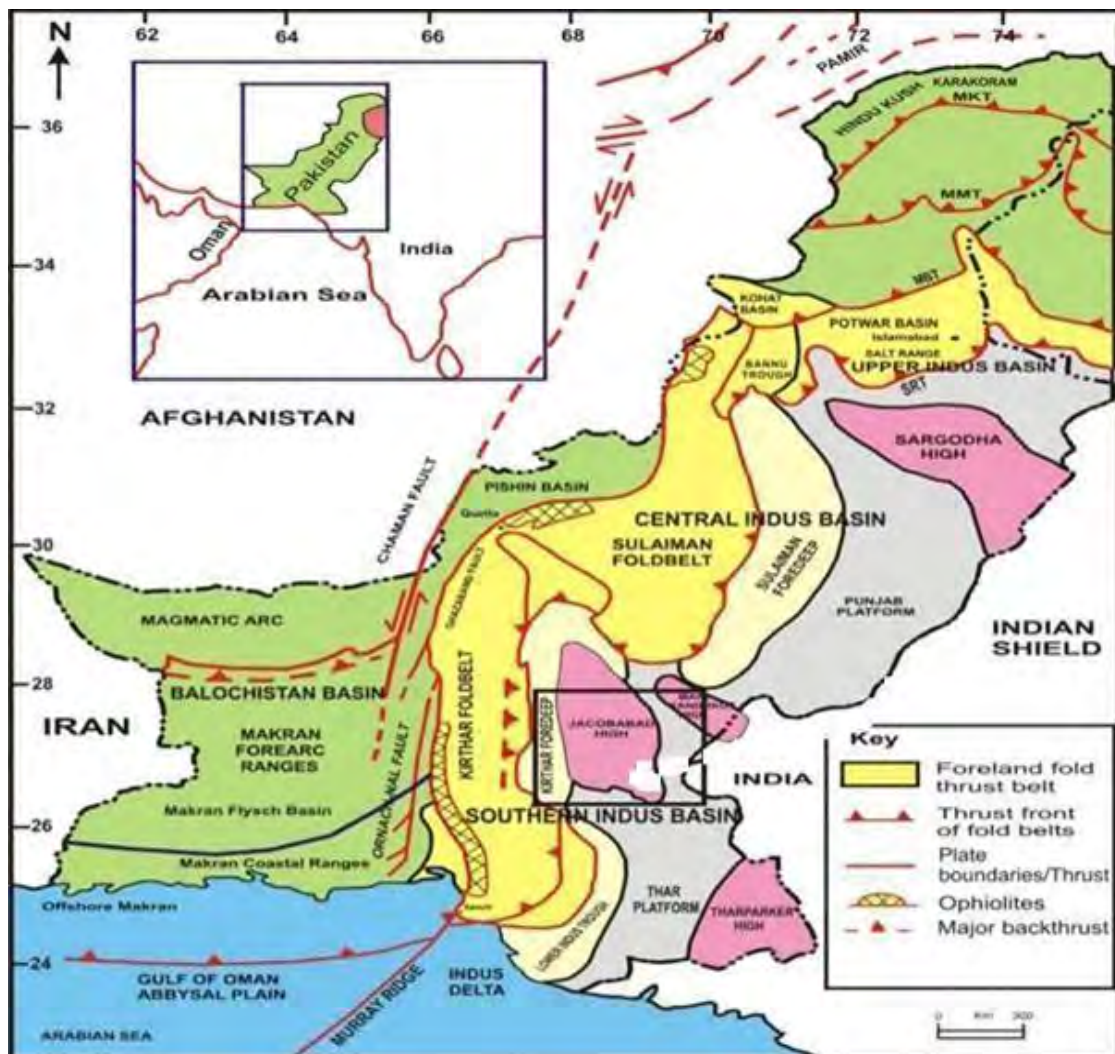


Figure 2.1: Tectonic and sedimentary basin of Pakistan (modified from Aziz & Khan, 2003), with the study area defined within the highlighted black box.

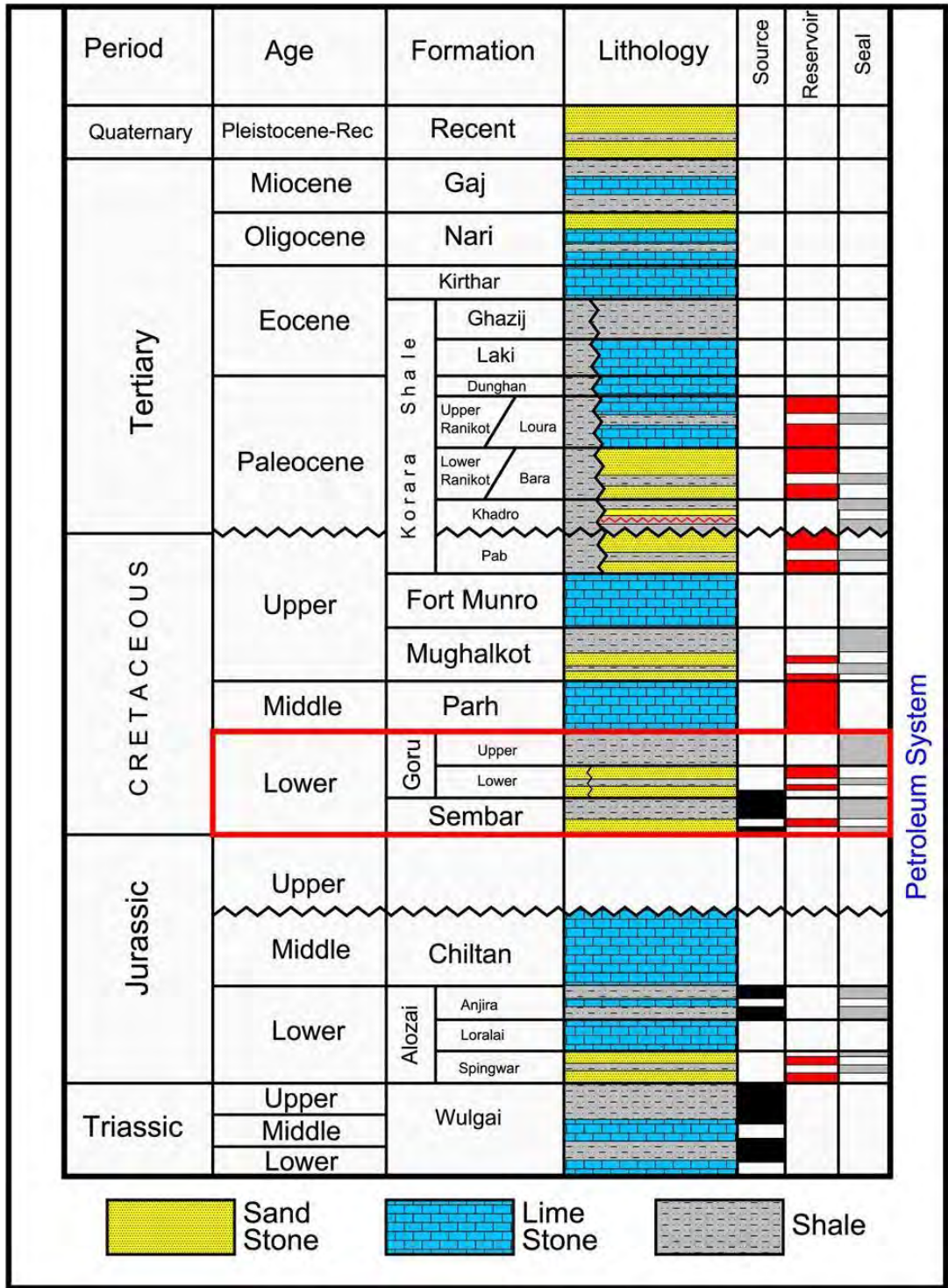


Figure 2.2: Schematic stratigraphic chart of the Lower Indus Basin, with the reservoir interval under study (C sand) part of the Lower Goru formation (modified from Abbasi et al.,2016).

2.5 Petroleum Play of Study Area

Before conducting any geophysical survey, identification of the petroleum play of the area is of key importance. Petroleum play is primarily based on the maturation of a source rock, expulsion, and migration of those hydrocarbons from the source rock, a reservoir rock that can store those hydrocarbons, and presence of a vertical and lateral seal rock to trap the hydrocarbons accumulated in place. A key factor that can be associated with this play is the geological age identification of the source rock maturation (Stoneley, 1995). Approximately 37% of hydrocarbon production is associated with the production from the Lower Indus Basin (Kadri, 1995).

2.5.1 Source Rock

Sembar formation mostly dominant with black silty shale, have interbedded siltstone and argillaceous limestone, of the Cretaceous age is a proven and regional source rock in the Lower and Central Indus Basin of Pakistan (Kazmi and Abbasi, 2008).

2.5.2 Reservoir Rock

The petroleum play of the Lower Indus basin has been mainly characterized by the Cretaceous age formations, with the sands of the Lower Goru formation serving as primary reservoir rock for hydrocarbon accumulation (Kadri, 1995). Lower Goru sands show an average primary porosity of around 11% in the study area (Kazmi and Rana, 1982).

2.5.3 Seal Rock

Reservoir rocks can accumulate hydrocarbons but with any other pathway they would leak out and migrate away from the reservoir rock, thus to trap and cut the access of hydrocarbons migration from reservoir rock, a presence of barrier or cap rock that acts as a seal rock, and in the lower Indus Basin, Upper Goru acts as a seal rock, but the parsequences of retrogradation and progradation during deposition of Lower Goru has deposited shale interbedding, so the mixed facies of Lower Goru formation containing shales also act as a seal rock to the sand reservoirs present in them (Kazni and Abbasi, 2008).

CHAPTER 03

3D SEISMIC DATA INTERPRETATION

3.1 Introduction

The building block to reservoir characterization stems from interpreting the seismic data set (Simm and Bacon, 2014). Seismic methods can be in simple terms be defined as the study of elastic sound waves that penetrate the earth's subsurface, using artificially sources, that work on the principles of reflection, refraction, and diffraction, and are governed by the acoustic impedance contrast of subsurface lithologies that result in the subsurface image. The resultant image is characterized as the two-way travel time image of these acoustic reflections. This information is integrated in cross-sections, which provide an image of the structure of the geological interfaces responsible for the reflection data are a bidirectional process. Subsurface modelling in which the seismic method is a key tool that can be coupled with seismic interpretation of the subsurface model are key in hydrocarbon industry. It is used to generate model and predictions about the properties and structure of subsurface. Seismic data interpretation has the objective to get or extract all subsurface information from the processed seismic data. Dobrin and Savit (1988) defined interpretation as: "The interpretation is the transformation of the seismic reflection data into structural picture by the application of correction, migration and time depth conversion."

3.2 Base Map

The generation of a base map is the initial step of the seismic interpretation in which the 3D data set of the Gambat-Latif block containing the navigation format of the In-line and crosslines were loaded along with the SEG-Y of these lines in the IHS Kingdom software, along with the wells, Tajjal South-01, Tajjal-02, and Tajjal-03 that is displayed in Figure 3.1.

3.3 Seismic to Well Tie

Seismic section although does provide an image of the subsurface yet marking of reflectors particularly the reservoir and source or the seal rock remains an ambiguity, considering not knowing the depth of the horizons, which can only be obtained from the well data, hence it is principal to tie the well with seismic, to obtain pivotal information about the horizons. Tying of well and

seismic does not only help in constructing the true geological sense of the study area, but also helps in constraining other parameters, such as wavelet extraction, zero phase checking etc., (Bacon et al., 2007; White, 2003; Liner, 2016; Simm and Bacon, 2014).

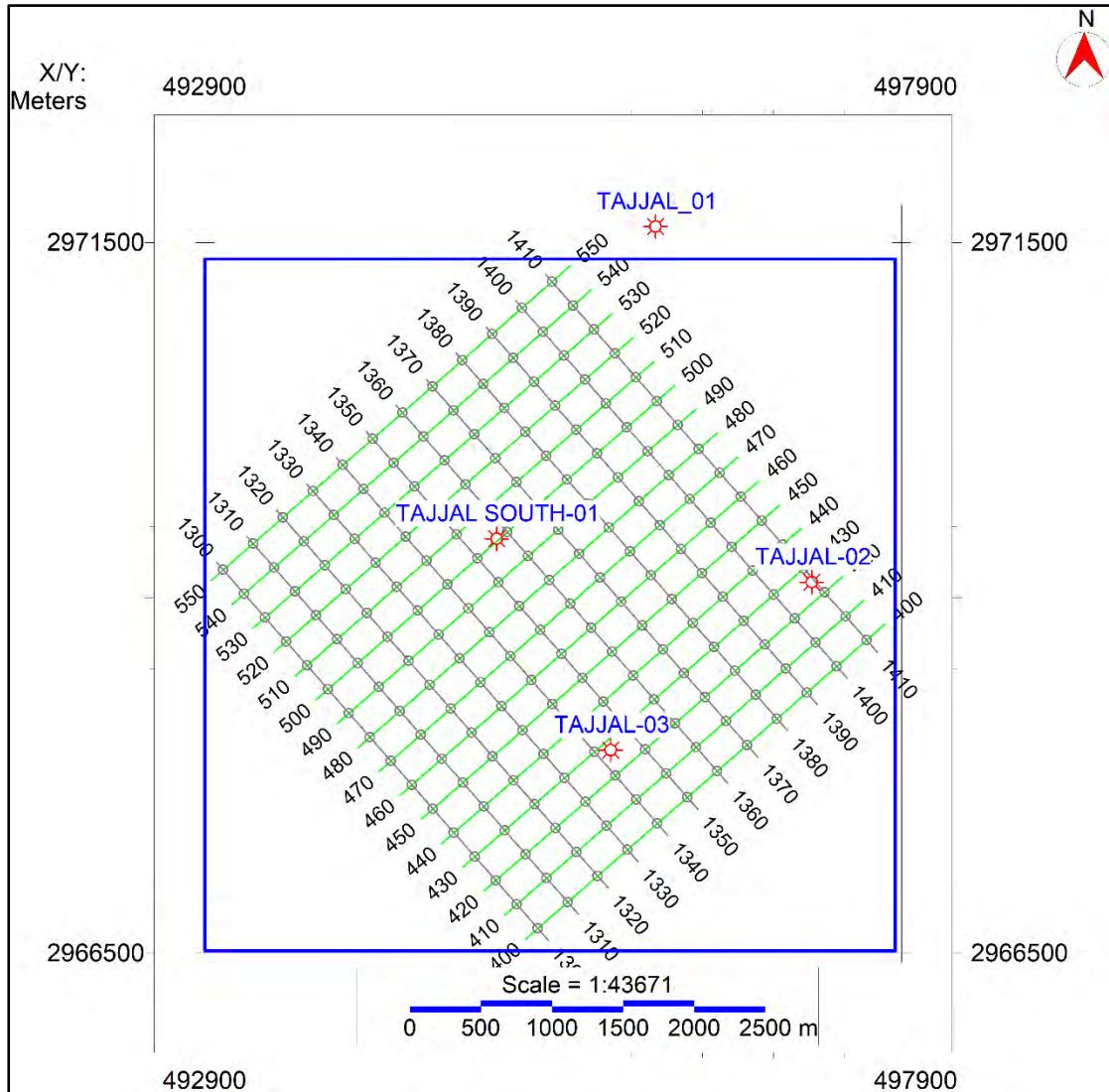


Figure 3.1: Spatial coverage of the seismic and well logs data utilized in the study, with the base map constructed on IHS Kingdom software, based on Universal Transverse Mercator 42N coordinate system.

Different methods are hence taken for this approach but the most utilized is the generation of a synthetic seismogram by obtaining the reflectivity from acoustic and density logs, from well data and convolving it with the extracted seismic trace spliced along the borehole. The synthetic seismogram produced in this study of TAJJAL-03 well is correlated with the seismic on inline 1336 displayed in Figure 3.2.

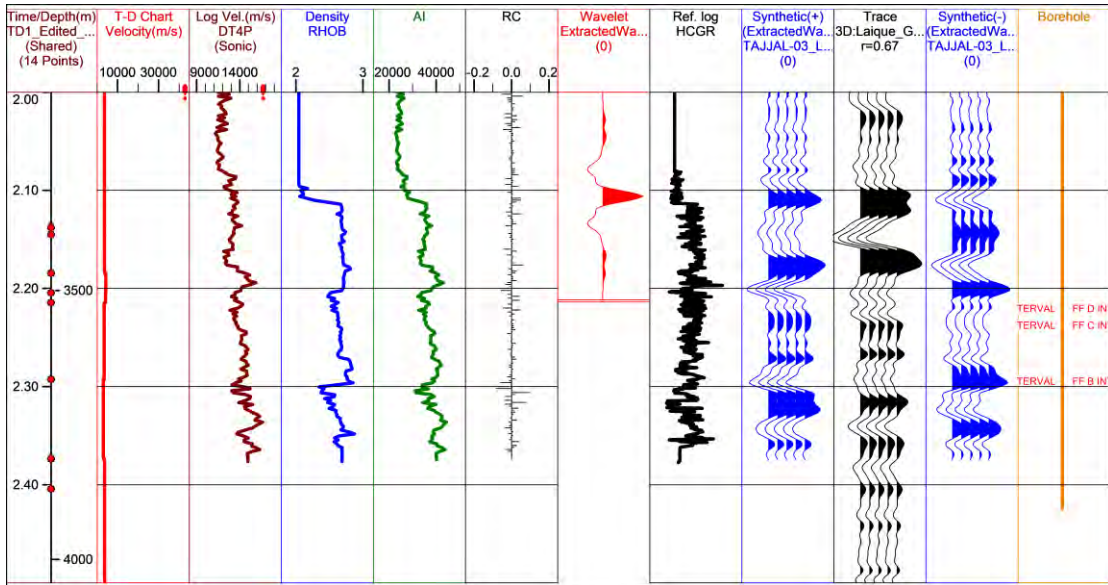


Figure 3.2: synthetic seismogram generated using the sonic and density logs from TAJJAL-03 las file, for the seismic to well tie between well log and seismic data. Horizons have been marked based upon this tie.

3.4 Faults Correlation and Fault Polygon Generation

Tectonics and geological trends are of key importance when defining the subsurface characteristics of the fault and interpreting them is crucial to identify reflector continuity and breakage. Since the study area lied in an extensional regime two major normal faults were discovered characterizing the block and were interpreted on many of the seismic inlines. These faults were then correlated and digitized to generate fault polygons, showing the direction of the faults present in the subsurface, and to characterize breakage of contours on fault polygons.

3.5 Horizon Identification

Seismic to well tie helps in correlation of the well the tops on seismic data, which in turn helps in marking the horizons on inlines and crosslines and correlating them for any Mistie to be removed while horizon marking (Onajite, 2013). Prominent reflectors are marked with the help of the synthetic seismogram and with the help of well data from TAJJAL-03. With correlation from synthetic seismogram attained the horizon marking is also carried out in the IHS Kingdom software, where horizons Lower Goru, D Sands, C Sands and B Sands are picked

with each horizon having a different color. A major observation recorded that the horst and graben structures and the horizons marked show an east to west trend of two-way travel time increase, thus showing that no antithetic fault system is observed in the data set and the structure gets deeper in the west, the interpreted section can be seen in Figure 3.3.

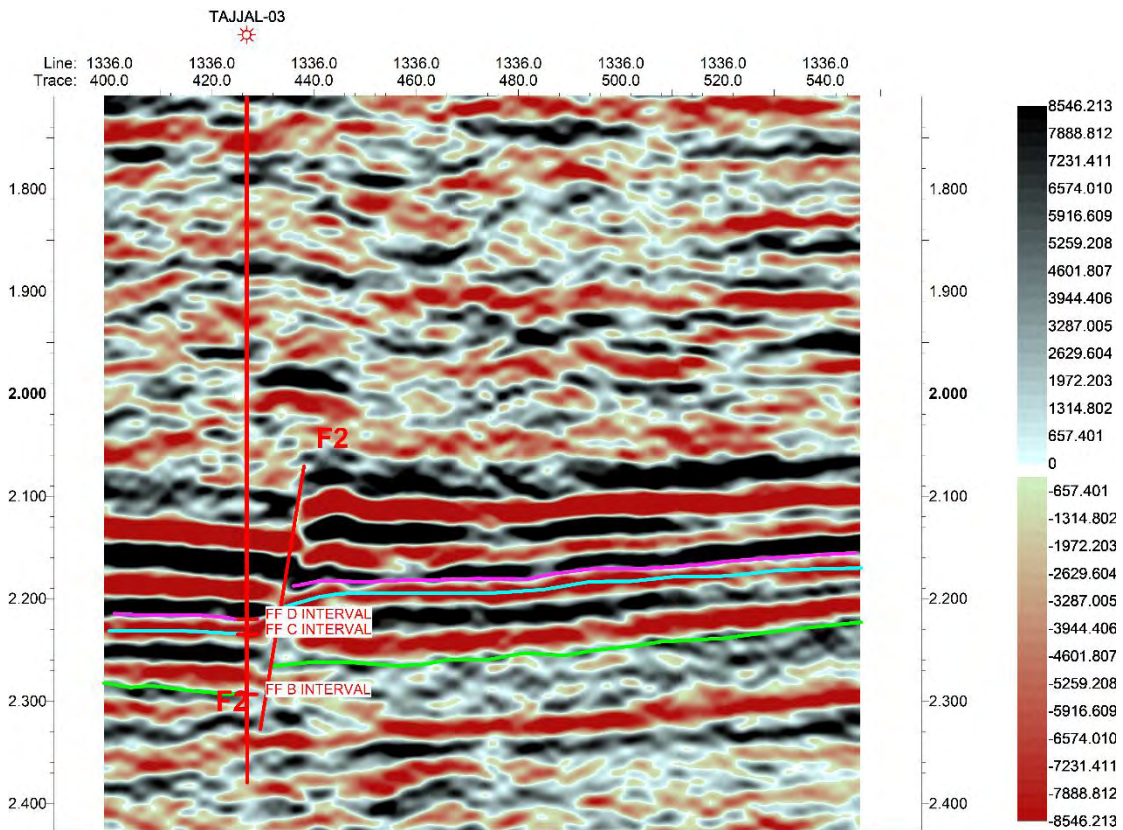


Figure 3.3: Inline 1336 with well displayed overlain by the trace obtained from seismic to well tie, marking the horizons as identified by synthetic seismogram on IHS Kingdom software.

3.6 Contour Map Preparation

Contour maps are prepared to generate contour lines that are marked by joining equal elevation, depth, time, or thickness. In the oil and gas industry and typically seismic studies, time, and depth contour maps hold key importance of revealing information. These time and depth contour maps are generated in a constrained grid over the picked horizons, with different interpolation algorithms utilized to interpolate time where there is no seismic information and continuing with the general trend of the structure. Since three seismic horizons were marked that were correlated with well and synthetic seismogram a grid was constructed

within the volume of the seismic cube and thus contour maps firstly of time and then later of depth were constructed.

3.7 Time Contour Map Interpretation

Time contours are prepared by joining points of equal time that have been picked through horizon picking of the reflectors, which explain about the position of horizon with respect to the travel time taken by the signal to be received on the receivers. Contours are really a basic and very significant tool to identify structures. Integrating the base map, picked horizons a time grid or the picked horizon level is generated and the two-way travel time contour maps for B Sands, C Sands, D Sands are generated which can be seen in the Figure 3.4 that shows the time variation of the B Sands with a contour interval of 0.01s and a time variation of 2.220s to 2.290s. Figure 3.5 shows the C Sands contour map with a contour interval of 0.01s and time variation of 2.17s to 2.23s, Figure 3.6 shows the D Sands time contour map and with a contour interval of 0.01s and time variation of 2.16s to 2.24s. The time variation that can be seen in the contour maps shows a trend of deeper structures present in the east, whereas the fault trend is in the NW-SE direction, the different colored polygons in the grid breaking the contour values are the fault polygons which were the three major faults identified as the subsurface structure.

3.8 Depth Contour Map Interpretation

Process of preparing a depth contour map is like that of time contour maps, but the technicality that differs it from time contour maps is that it utilizes the time of the horizons that were picked and using well data information about the velocity of the lithologies, converts the time values into an approximated depth of the lithology depending on the interval velocity function chosen for accurately marking the depths. After the horizons are converted from time to depth then a depth grid is prepared of the picked horizon level of B Sands, C Sands, D Sands displayed in Figures 3.8, 3.9, and 3.10 respectively Figure 3.8 shows the B Sands depth contour map where the contour interval was taken at 20m and the depth variation ranges from 3560m to 3660m, while Figure 3.9 shows the C Sands depth contour map with contour interval of 16m and depth variation from 3476m to 3496m. Figure 3.10 shows the C Sands depth map with a 16m contour interval

and depth variation from 3360m to 3440m. The depth and thickness of the horizons increases in the eastward direction, that can be associated the faults in the east are relatively new faults that emerged in contrast to the westward faults that are rather geologically older.

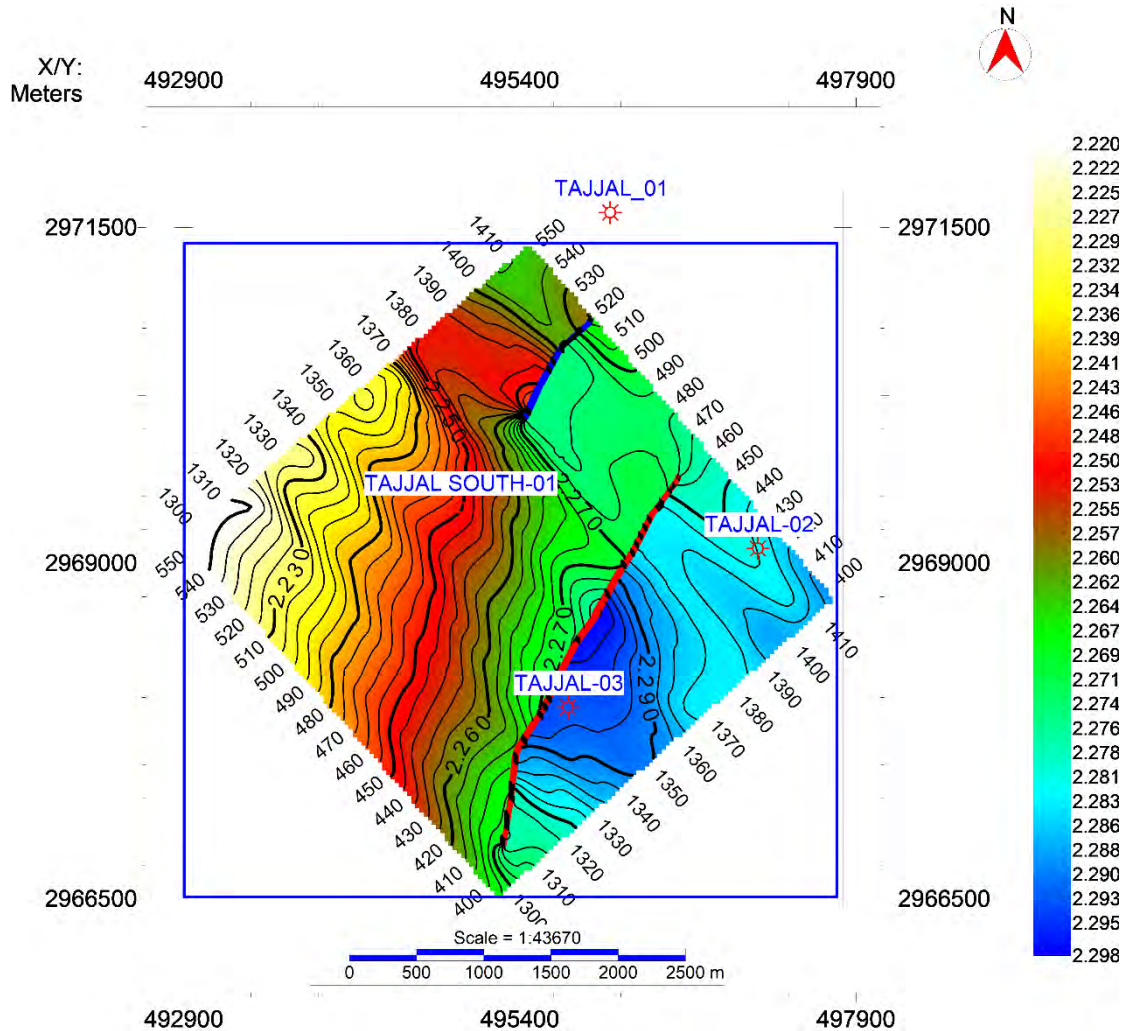


Figure 3.4: Time contour map of B Sands with a contour interval of 0.01s, spatially distributed on the base map with a maximum of 2.290s and minimum of 2.220s, created on IHS Kingdom software.

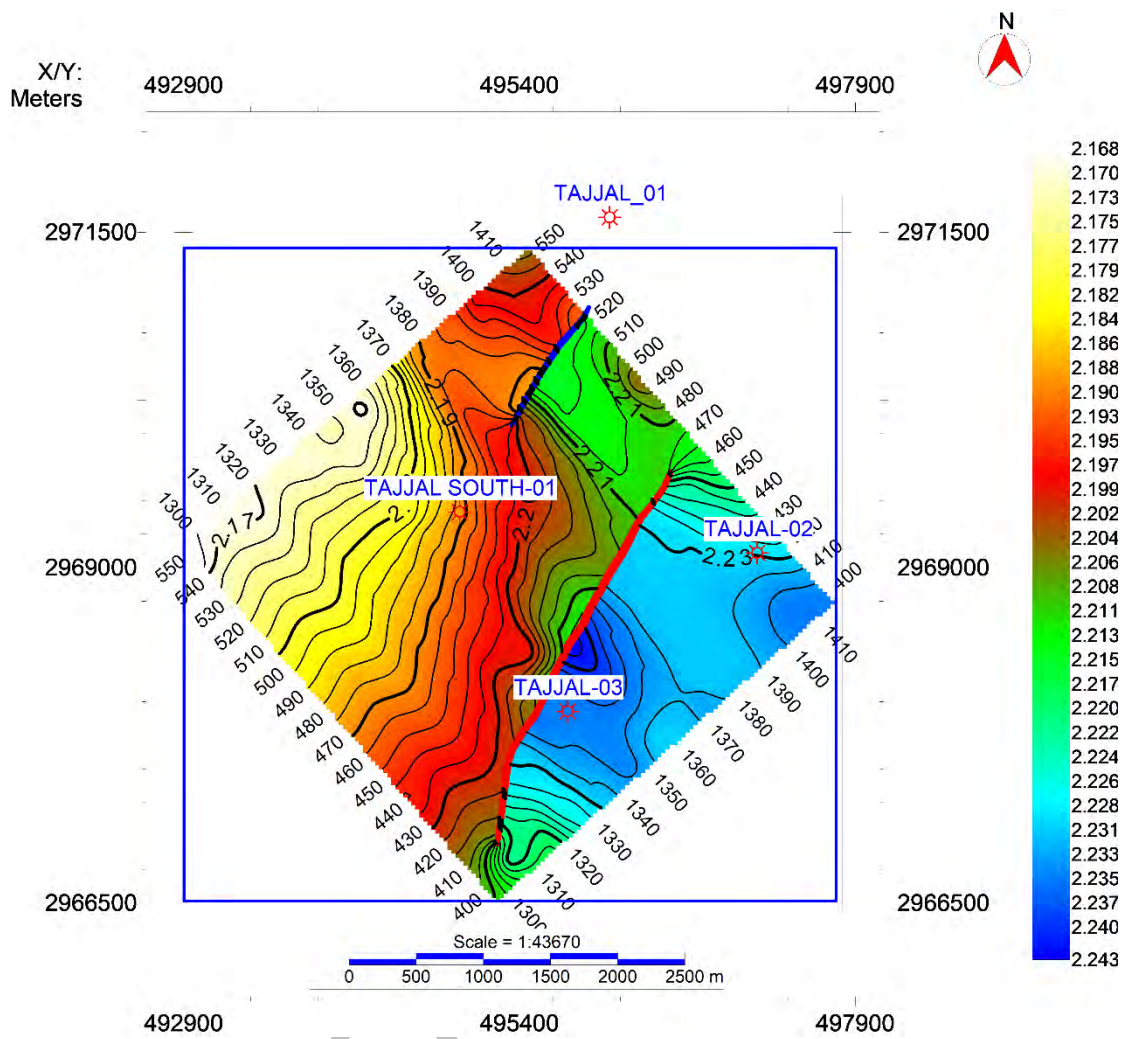


Figure 3.5: Time contour map of C Sands with a contour interval of 0.01s, spatially distributed on the base map with a maximum of 2.23s and minimum of 2.17s, created on IHS Kingdom software.

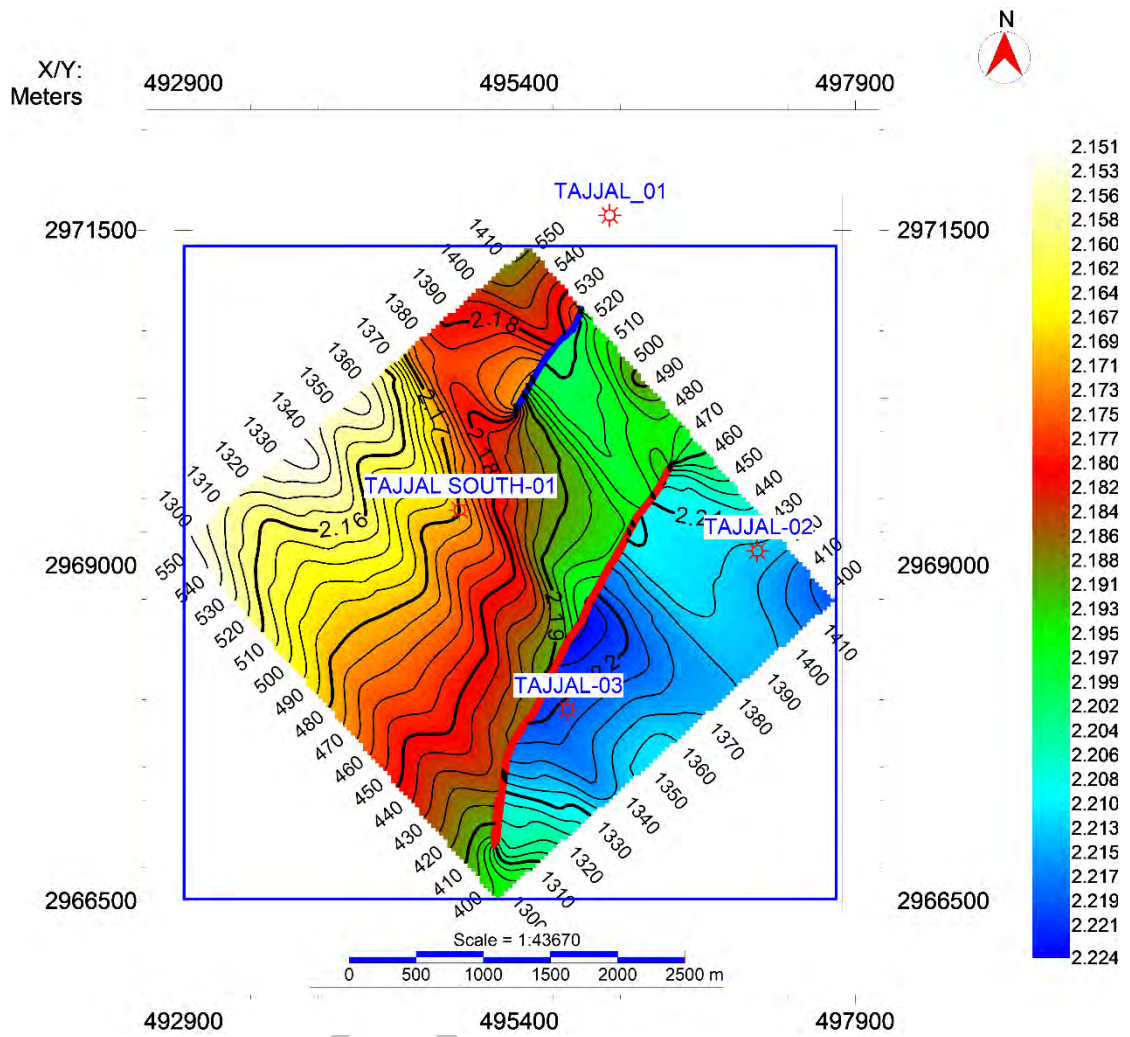


Figure 3.6: Time contour map of D Sands with a contour interval of 0.01s, spatially distributed on the base map with a maximum of 2.24s and minimum of 2.16s, created on IHS Kingdom software.

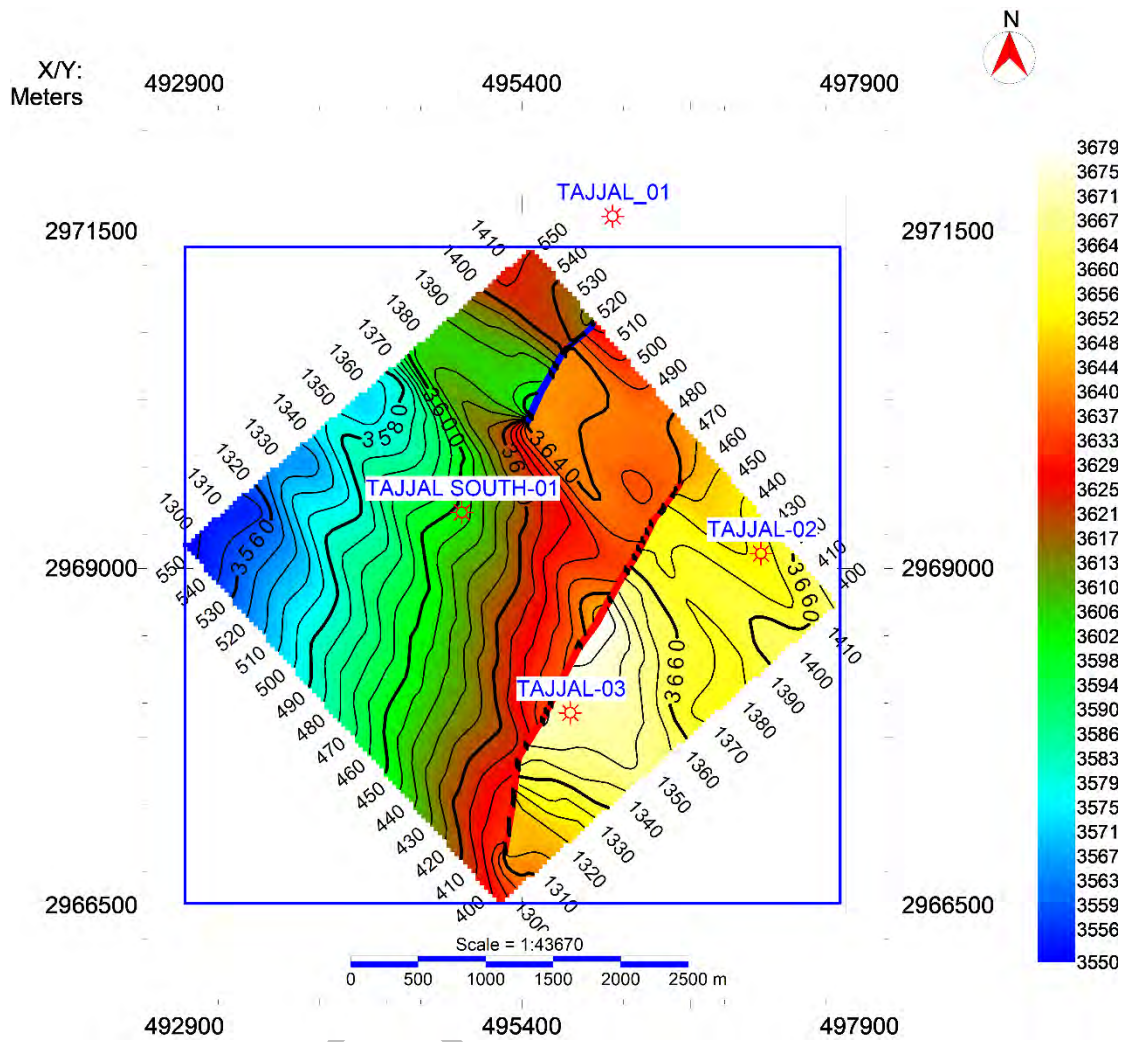


Figure 3.7: Depth contour map of B Sands with a contour interval of 20m, spatially distributed on the base map with a maximum of 3660m and minimum of 3560m, created on IHS Kingdom software.

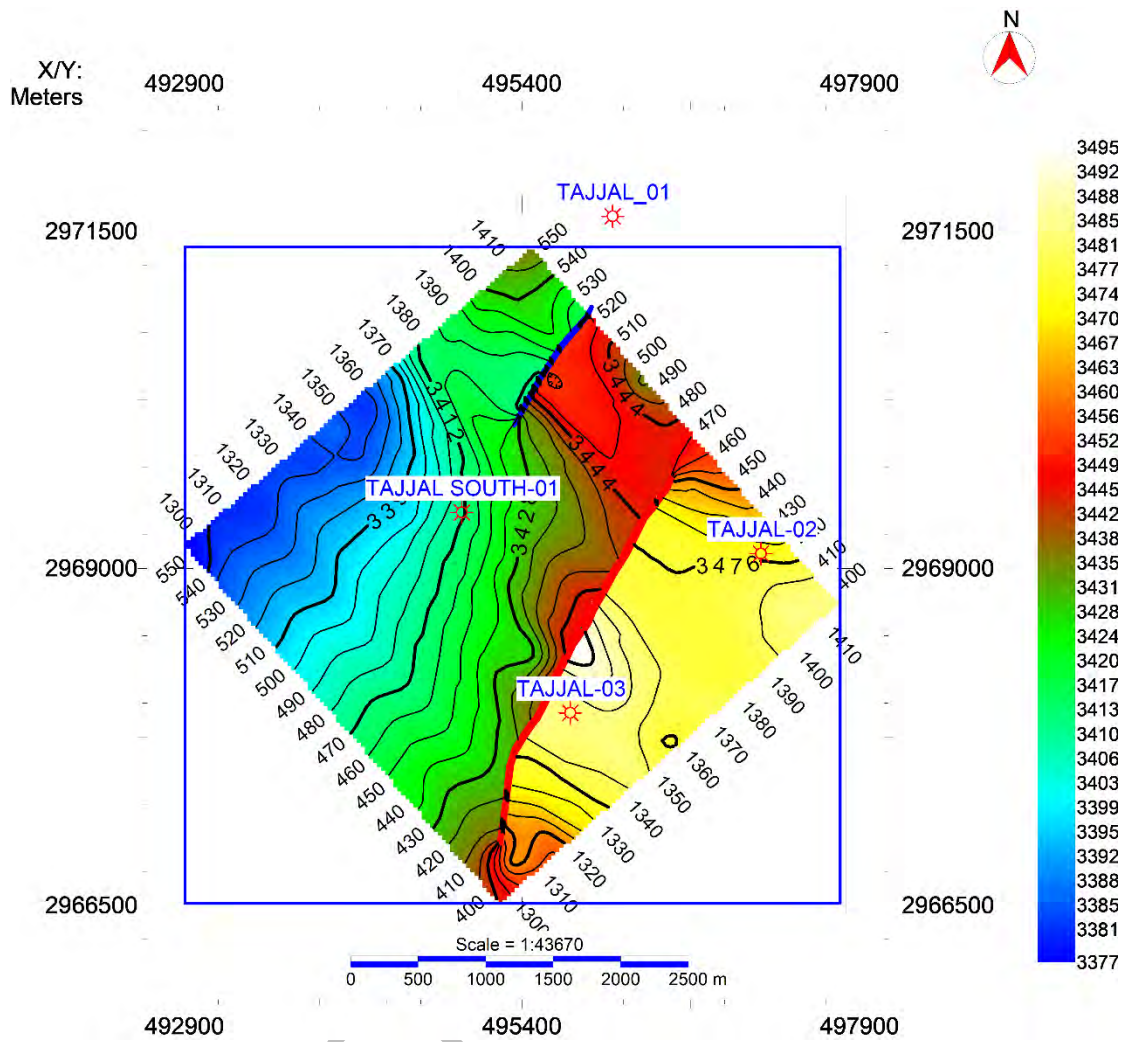


Figure 3.8: Depth contour map of C Sands with a contour interval of 16m, spatially distributed on the base map with a maximum of 3496m and minimum of 3476m, created on IHS Kingdom software.

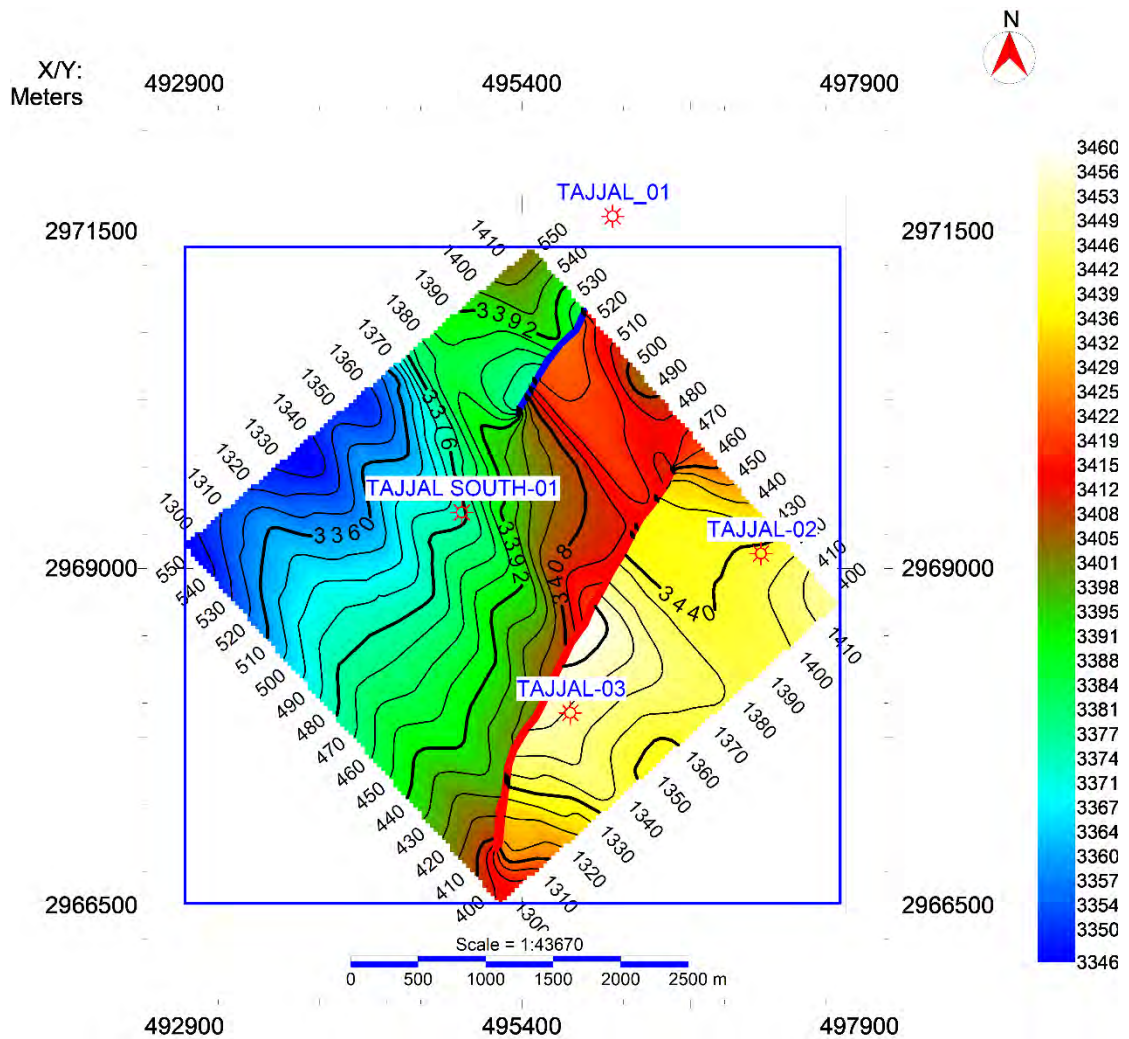


Figure 3.9: Depth contour map of D Sands with a contour interval of 16m, spatially distributed on the base map with a maximum of 3440m and minimum of 3360m, created on IHS Kingdom software.

3.9 Seismic Attributes Analysis

Any information extracted either by direct measurements from seismic data or by indirect experience and logic-based reason is seismic attributes. Since the advent of seismic attributes in 1970s it has gained considerable popularity for qualitative interpretation, lithology and fluid detection and reservoir characterizations. The study of seismic attributes provides us with qualitative interpretation about the geometry and physical properties of sub surface. The amplitude content of seismic data in frequency domain gives us information about the physical parameters of seismic wave like acoustic impedances of earth layers, reflection coefficient, velocities, and absorption coefficient etc. A phase spectrum is the principal component in finding the shape of the reflector and the geometric configuration. The generic objective of applying seismic attributes to our seismic data is to provide right and elaborated information to

Geophysicist about structure, stratigraphy, and other properties of the acquired data (Chopra and Marfurt, 2005).

Attributes are classified into different types by different authors. Below is the classification of attributes based on the characteristics of different domains.

3.9.1: Pre-Stack Attributes

CDP gathers are given as input data in pre-stack attributes. Pre-stack attributes have azimuthal and angle related information. Pre-stack data have large volume of data, but they contain valuable information about fluid contents and fracture sets propagation. AVO (Amplitude Verses Offset), Velocities and Azimuth related attributes are included in pre-stack attributes.

3.9.2: Post Stack Attributes

CDP stacked data is given as input in post stack attributes. The term stacking refers to an averaging technique in which angle or offset and azimuth related information is not preserved. Seismic post-stack attributes are most capable when dealing with huge data for initial reconnaissance study. For detailed investigation seismic pre-stack attributes are applied.

Attributes classified based on relation to geology are:

3.9.3: Physical Attributes

Spatial and temporal variation of geological properties is described by physical attributes related to physical qualities and quantities. Physical attributes are commonly used for lithology identification and characterization of reservoirs. Like the trace envelop, magnitude is related to acoustic impedance, frequency is influenced by bed thicknesses.

3.9.4: Geometrical attributes

The spatial and temporal variation of geological properties is described by geometrical attributes. Like lateral-continuity attribute measured by semblance algorithm is indicator of identical beds as well as discontinuity in bedding. Stratigraphic interpretation can also be done by geometrical attributes as such attributes can define different events, characteristics, and spatial relationships (Taner, 2001).

3.9.5: Instantaneous-Dip Attribute

The attribute applied on seismic in-line 1384 time slice extracted at 2.3 seconds is of Instantaneous dip attribute shown in figure 3.11. Faulted zones show high dips on seismic section and faults can also be identified easily on time slice with blue color whereas the low dip area away from faulted zone show low dip values.

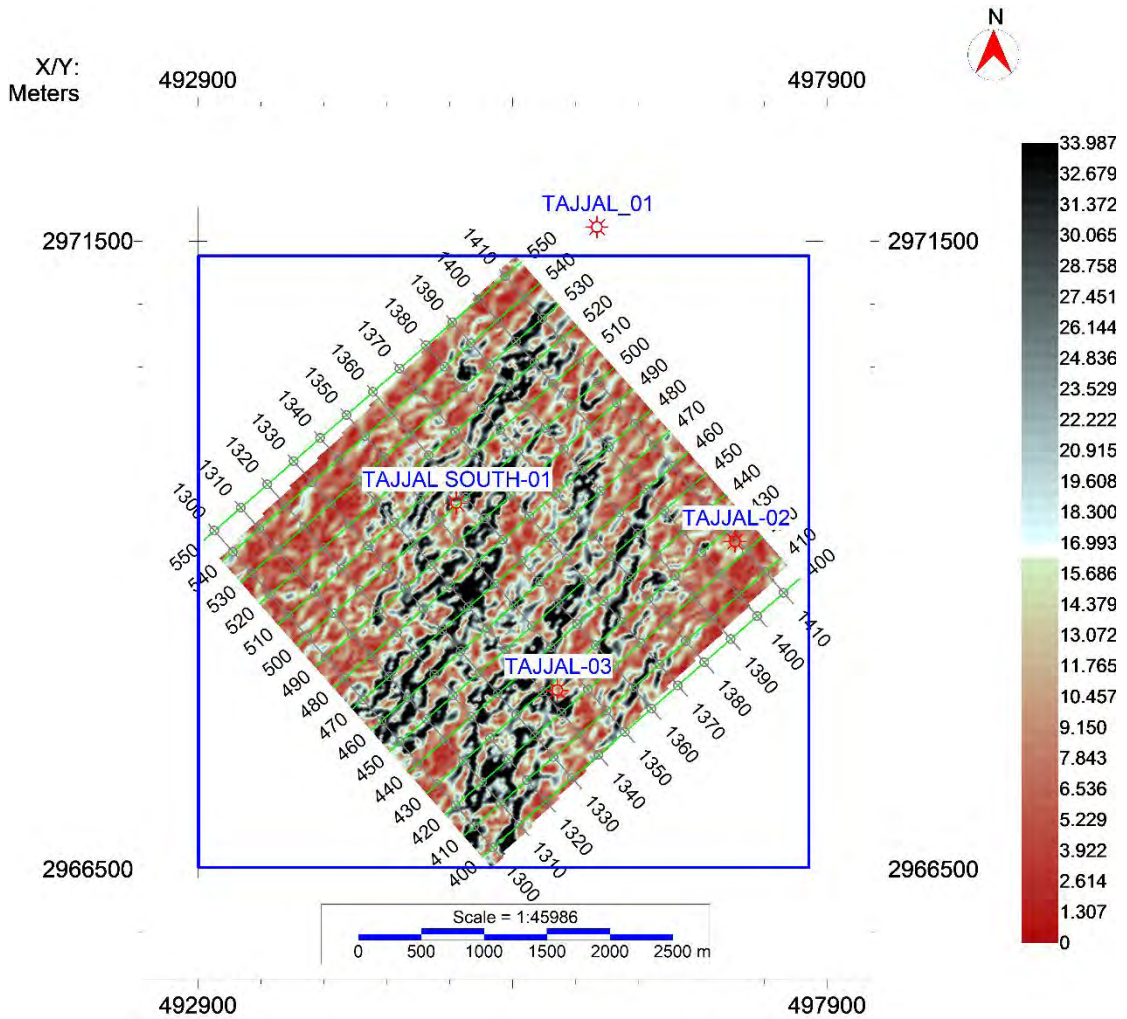


Figure 3.10: Time slice of Instantaneous dip attribute at 2.3 seconds.

3.9.6: Shale Indicator

Shale attribute is a hybrid attribute that combines several primitive attributes to detect possible shale beds in a possible clastic environment. Shale beds are thin and have high lateral continuity due to their depositional setting. Shale indicator is the combined output attribute of instantaneous frequency or wave number, parallel bedding indicator, similarity, and variance attribute. Shale indicator attribute can be interpreted as:

- The higher the output values, the higher the possibility of shale and lower the value greater the possibility of other rocks such as sands and carbonates.
- Seismic time slice at 2.4 seconds shows maximum value of shale presence shown in figure 3.11.

(www.rocksolidimages.com/attributes; www.ihskingdom.com/mathematics-behindshale-indicator-attribute/)

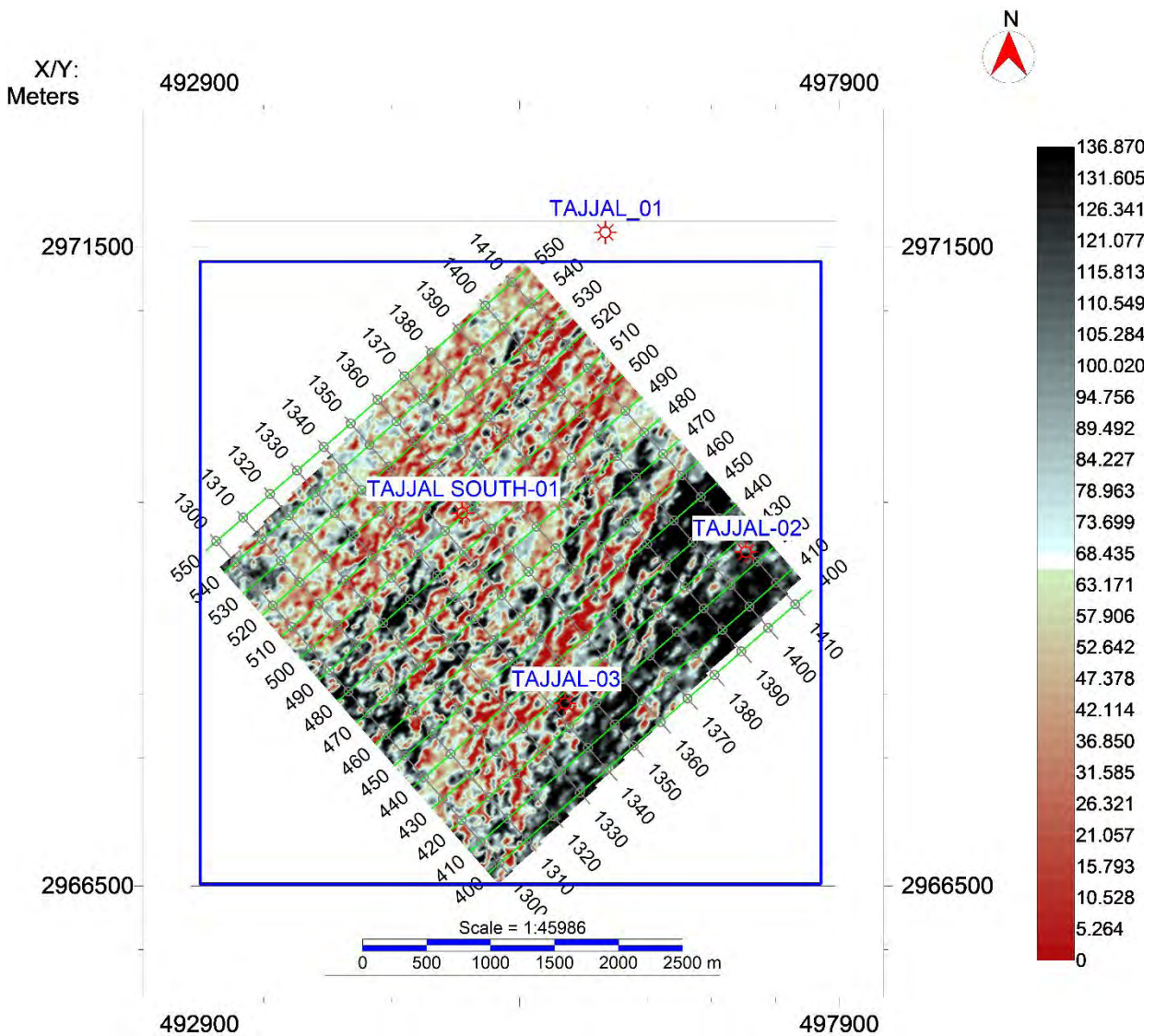


Figure 3.11: Time slice extracted for shale indicator at 2.4 seconds.

Hence, various rocks solid attributes applied on the seismic data confirms our structural interpretation and gives direct additional information about presence of faults, reservoir rock, fluids, and existence of shale layering.

CHAPTER 04

PETROPHYSICAL ANALYSIS

4.1 Introduction

Well logging is a tool to measure the subsurface properties of earth. The physical and the chemical properties of the rock explained the existence and behavior of the rocks, fluids, and soils (Rider, 1996). Well logs used by the Petro physicist are caliper, resistivity (LLD), sonic (DT), gamma ray (GR), neutron (NPHI), and density (RHOB) logs etc., and all other desired information is obtained from these logs. The significance of each log cannot be ignored as they play vital role in quantifying reservoir parameters such as porosity, net pay zone, fluid content, and shale volume. Petrophysical interpretation generally has little concern with seismic, while offers detailed information about borehole measurements, ultimately contributing to reservoir characterization (Asquith et al., 2004).

4.2 Reservoir Petrophysical Properties

Petro physicists compute reservoir petrophysical properties, which include the following.

4.2.1 Lithology

Geoscientists can use log measurement results like gamma, neutron, density, photodiodes, resistivity, as well as their combined effect to determine the lithology down hole when merged with local geology and core study.

4.2.2 Porosity (ϕ)

How much of the rock's pore (or fluid-occupied) space is occupied, this is typically determined using a device that gauges the rock's response to neutron or gamma ray bombardment. Rock porosity can also be determined and measured using NMR logs and sonic wave speed.

4.2.3 Water Saturation (S_w)

Water saturation is the percentage of pore space that is filled with water. Typically, the resistivity of rocks is measured using instruments.

4.2.4 Hydrocarbon Saturation (Sh)

Hydrocarbon saturation is a measure of how much pore space is occupied by hydrocarbons. Usually, this is calculated by deducting the water content from that one.

4.2.5 Net Pay

Rock thickness that can efficiently deliver hydrocarbon into the well bore.

4.3 Classification of Geophysical Well Logs

Well log is a profile showing different properties of formation, which are measured through wells. Every log gives some information about the subsurface. Some logs are correlated with other logs to assure our prediction of lithologies. Geophysical well logs can be classified into three categories.

- Lithology logs
- Resistivity logs
- Porosity Logs

4.3.1 Lithology Logs

Lithology logs are mostly used to identify the boundaries between permeable and impervious layers, extracted information about permeable formations assist in correlation with other wells. Lithology logs are caliper (CALI), spontaneous potential (SP) and gamma ray (GR).

a) Caliper (CALI) Log

Caliper log is used to determine the diameter of the borehole. Moreover, it provides detailed information about the formation's cavities portraying loose lithology along with presence of dense rocks where caving is absent. In porous layers, formation of mud cake reduces the diameter of borehole and these variations in diameter influence the logs measurements (Bjorlykke et al., 2010).

b) Gamma Ray (GR) Log

The use of gamma-ray logs allows for the measurement of a formation's natural radioactivity, also known as lithology logs. The

radioactive materials have high concentration in shale while shale free sand and carbonates have low gamma-ray reading.

Volume of Shale (Vsh)

The GR log's linear method for calculating the shale volume or the gamma ray index, be calculated from equation 4.1.

$$IGR = \frac{GR_{log} - GR_{min}}{GR_{max} - GR_{min}} \quad (4.1)$$

where, GR_{log} is the gamma ray values that are taken as input from the log, Gr_{min} is the minimum value of GR in the anomalous zone, whereas Gr_{max} is the maximum value of the GR in the ambiguous zone.

c) Spontaneous Potential (SP) Log

In the absence of any externally applied current, the borehole's natural or spontaneous voltage difference from the surface is measured by the spontaneous potential log. It is a very straightforward log that only needs a reference electrode above the surface and an electrode inside the borehole. These spontaneous potentials result from electric charge in the downhole and formation fluids having a different access to different formations, which results in a spontaneous current flow and, in turn, a spontaneous potential difference. Four main uses of this log are:

- Delineation of permeable formations.
- To determine the resistivity of water.
- Indicating shale within a formation.
- Correlation of wells and formation.

4.3.2 Resistivity Logs

Resistivity logs provide details about formation thickness, accurate value for the true formation resistivity and used for correlation purposes. Resistivity logs are mapped on the logarithmic scale due to wide variation in resistivity (0.2 to 2000 ohm) with depth.

Resistivity well logs are:

- Deep latero-log (LLD)
- Shallow latero-log (LLS)

a) Deep Latero-log (LLD)

Deep latero-log also termed as electrode log, mostly incorporate in measuring saltwater muds filled boreholes resistivity (Rmf). The surveying current basically controls the effective depth of this log investigation (Asquith et al., 2004).

b) Shallow Latero-log (LLS)

Shallow latero-log measures resistivity of fluids presents in invaded zone (Rt). In water bearing zone, the Shallow latero-log determines a low resistivity because mud filtrate resistivity (Rmf) is almost equal to mud resistivity (Rm) (Asquith et al., 2004).

4.3.3 Porosity Logs

Porosity logs are used to measure water saturation in a formation, furthermore, they provide reliable information about lithology and porosity along with discrimination of oil and gas carrying zones.

Porosity well logs are:

- Sonic/Acoustic (DT)
- Neutron Porosity (NPHI)
- Density (RHOB)

a) Sonic /Acoustic (DT) Log

Sonic logs measure the interval transit time or DT (Δt) of the sound wave compression passing through the formation. The formation's porosity and Sands transit time are related. The interval transit time is related to the porosity of the formation. The unit of measure is microseconds per foot (Asquith et al., 2004). Porosity of the formation can be calculated by using equation 4.5.

$$\Delta_s = \frac{\Delta_{tlog} - \Delta_{tm}}{(\Delta_{tf} - \Delta_{tm})} \quad (4.5)$$

where, Δ_s represents the calculation that is derived from the sonic log, Δ_{tm} is the interval transient time of the matrix, Δ_{tlog} is the interval transit time of formation represents the transient time of the fluid (salt mud=185 and fresh mud=189). The interval transient time of the formation depends upon the matrix material, its shape, and cementation (Wyllie et al., 1956). If fluid (hydrocarbon or water) is present in the formation, transient interval time is increased, and this behavior

shows an increase in porosity which can be calculated by using sonic log (Asquith et al., 2004).

b) Neutron Porosity (ϕ_n) Log

The neutron porosity log is known as porosity log; basically, it is used to calculate or determine the hydrogen ion (HI) concentration in the formation (Asquith et al., 2004). The neutron log gives value of water filled porosity if the shale free formation is filled with water. In gas reservoirs, porosity measured by the neutron log is low then formation true porosity as the hydrogen ions concentration is less in gas reservoir than that of oil and water (Asquith et al., 2004). It is the one limitation of neutron log that is known as the gas effect.

c) Density (RHOB) Log

This log is also known as porosity log that is used to measure electron density of the formation, (Asquith et al., 2004). Formation electron density is relative to bulks density of formation. The density logs are used with other logs and separately or for different purposes (Tittman and Wahl, 1965).

Density logs can be used to find out the correct porosity of the formation (Asquith and Gibson, 2004). By using equation 4.6, density porosity can be calculated as

$$\Phi_d = \frac{\rho_m - \rho_b}{\rho_m - \rho_f}, \quad (4.6)$$

where, ρ_d represents porosity derived from the density log, ρ_b represents bulk density of formation derived from the RHOB log, ρ_m represents matrix density, and ρ_f represents the density of fluid. The main purpose of present petrophysics is to obtain calculation about porosity, saturation of water and hydrocarbon.

4.4 Average Porosity (ϕ_{avg})

The total porosity is calculated by adding all three porosity values. Average porosity can then be calculated to get the effect of all the pores. Average porosity is measured by adding neutron porosity and density porosity values. Whereas the number of interconnected pores give effective porosity. The calculation of average porosity can be done by using equation 4.7.

$$\Phi_{avg} = \frac{\phi_d + \phi_n}{2}, \quad (4.7)$$

where, ϕ_{avg} is average porosity, ϕ_d is density porosity and ϕ_n is neutron porosity.

4.5 Effective Porosity (ϕ_e)

"The proportion of the interrelated pores to the overall amount of the rock" is how it is described.

The shale effect is removed from the rock unit." The zone, which is rich in shale, effective porosity would be zero. Effective porosity is used to mark the saturated zone. The effective porosity can be calculated by equation 4.8 (Asquith and Gibson, 2004).

$$\phi_e = \phi_{avg} * (1 - V_{sh}) \quad (4.8)$$

where, ϕ_e is the effective porosity which is to be calculated and ϕ_{avg} represents the average porosity.

4.6 Water Saturation (S_w)

The proportion of a rock's pore volume that is filled with water during formation is known as water saturation. If the presence of hydrocarbons in the formation's pores is not confirmed, it is presumed that they will be filled with water. One of the fundamental purposes of well logging is to establish the saturation levels of water and hydrocarbons. To calculate saturation of water in the formation, a mathematical equation known as the Archie equation is used, which is given below as equation 4.9.

$$S_w = n * \sqrt{\frac{(F * R_w)}{R_t}} \quad (4.9)$$

F is the formation factor where $F = a/m$, where R_w is the water resistivity, R_t is the true forming resistivity used in laterolog deep (LLD) applications, n is the saturation exponent, which ranges in value from 1.8 to 2.5 and therefore is taken as 2, a is consistent and its value is assumed to be 1, is the effective porosity, and m is the cementation factor, which is taken to be 2. All the other parameters to calculate R_w can be calculated from spontaneous potential logs in the following steps.

1. Pick SSP from SP log by using formula given in equation 4.10 (Rider, 1996)

$$SSP = SP_{CLEAN} - SP_{SHALE} \quad (4.10)$$

SSP = Static spontaneous potential

SP_{CLEAN} = Spontaneous potential for sand

SP_{SHALE} = Spontaneous potential for shale

2. Determine the formation temperature FT against the depth of the reservoir formation using the equation 4.11 (Rider, 1996)

$$FT = \frac{(BHT - ST) * FD}{TD} \quad (4.11)$$

FD = Formation depth

BHT = Bottom hole temperature

ST = Temperature at surface

TD = Total depth of the borehole

3. Resistivity of the mud filtrate that is measured at surface temperature $0.17 \Omega m$ is used to calculate the resistivity of mud filtrate at zone of interest calculated by equation 4.12.

$$R_{mf2} = \frac{(ST + 6.77) * R_{mf1}}{(FT + 6.77)} \quad (4.12)$$

ST = Temperature at surface

FT = Formation Temperature

R_{mf1} = Resistivity of mud filtrate measured at surface temperature

4. The next step is to calculate the resistivity of the mud filtrate but for that if R_{mf2} is greater than $0.1 \Omega m$ then R_{mfe} is calculated by equation 4.13.

$$R_{mfeq} = 0.85 \times R_{mf2}, \quad (4.13)$$

If R_{mf2} is less than $0.1 \Omega m$ then we use chart SP-1 (Schlumberger Chart) given in appendix-2 to derive a value of R_{mfe} at formation temperature, as shown in the Figure 4.1. The second bar in the figure

contains the R_{we} values and using the values of SSP, FT and R_{mfe} , R_{we} value is calculated which is $0.0048 \Omega m$.

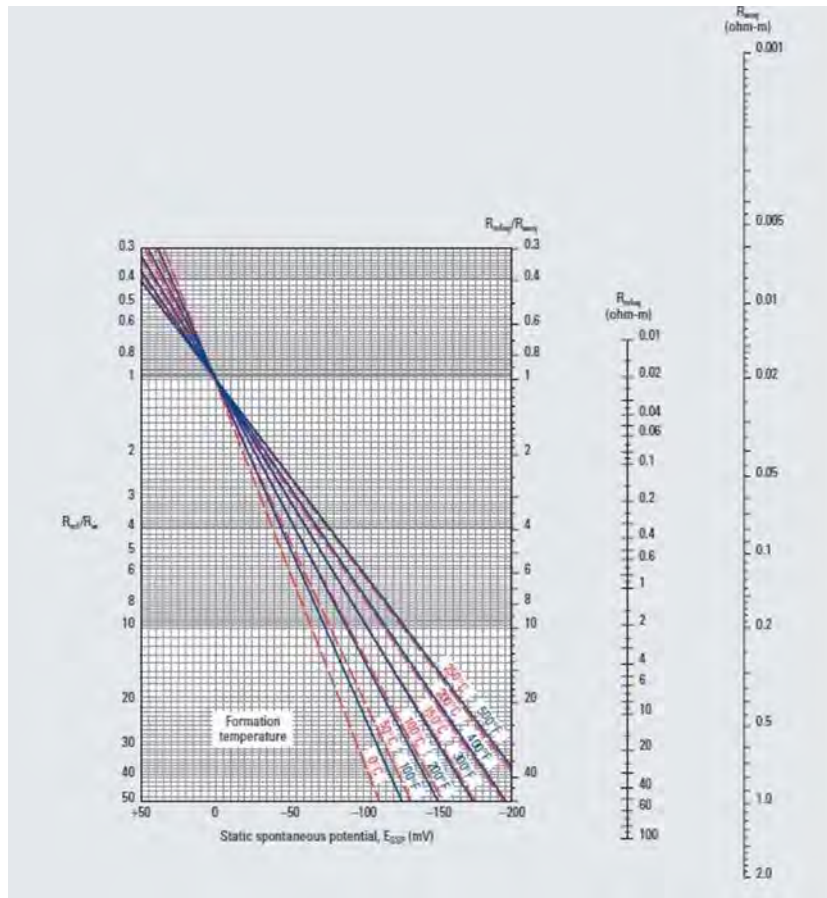


Figure 4.1: Determination of R_{weq} from SP-1 chart uses the well data header file to find resistivity of water equivalent of water (Schlumberger, 1989).

5. The last step is to calculate the value of R_w after obtaining the value of R_{we} from the SP-1 chart, so we use FT and R_{we} values and use the SP-3 chart to calculate R_w , given below in Figure 4.2.

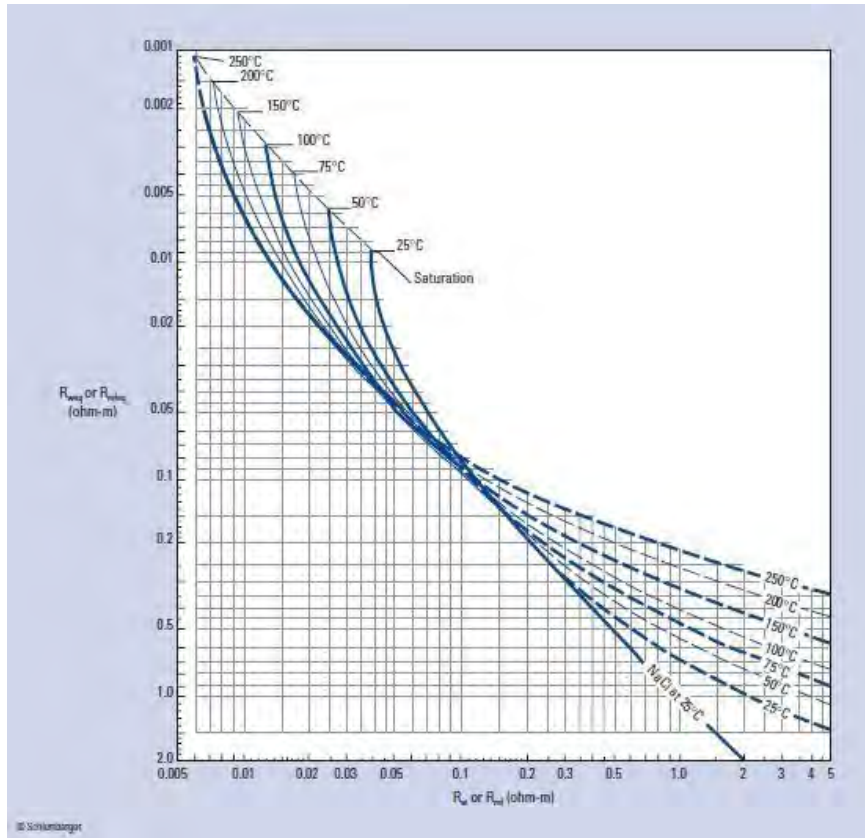


Figure 4.2: Determination of R_w from SP-3 chart after determining R_{weq} and using formation temperature curves can be utilized to determine where R_w for given well fits best (Schlumberger, 1989).

The resistivity of water calculated for C Sands sands is $0.016 \Omega m$, after calculating all these parameters we use these values in Archie equation for calculating the saturation of water.

4.7 Hydrocarbon Saturation (S_h)

Hydrocarbon saturation can be defined as “the pore in the formation is filled with hydrocarbon.” Equation 4.14 is used to calculate the hydrocarbon saturation.

$$S_h = 1 - S_w \quad (4.14)$$

Where,

S_w represents the water saturation,

S_h represents hydrocarbon saturation.

4.8 Interpretation of Well Logs

Interpreting well logs with a few indications is a very easy task, but that is if there is no inconsistency in the data set or any flaw in the borehole geometry, with issues such as borehole breakouts, rugosity effect, or cavings that may occur

in unconsolidated lithologies to cause erroneous interpretations. For this instance, the stability of caliper log is of crucial importance especially in the reservoir formation. Power-log software was utilized to interpret the well logs of Tajjal-02 well. Although common utilization of the GR log is to determine the reservoir as clean or dirty, if the GR log is not present, then the use of SP log is rather a secondary piece of information that determines sands from shales. The separation of the LLD and LLS logs indicates fluid variation within the reservoir, with a higher separation indicative of gas, and smaller separation shows presence of oil respectively, with both showing higher resistivity. Porosity logs such as NPHI and RHOB also serve as clear hand indications of presence of porosity and fluid in the formation, such that both the logs decrease and since are placed in the same track and in reverse condition, with decreasing values form a crossover, that coupled with separation of LLD and LLS logs, provide first indications of presence of hydrocarbons. GR log can be further used to detect volume of shale, and a cut-off of 40% can further distinguish the sand and shale facies in the reservoir formation. Values below this cut-off indicate presence of sand and values higher than this can indicate presence of shales.

Petrophysical analysis on the Lower Goru formation's C-Interval on Tajjal-02 well showed two zones, first Zone is at a depth of 3724m to 3737m and Second Zone is at a depth of 3748.75m-3756.63m and of potential hydrocarbon accumulation with clear indicatives and are characterized below in Table 4.1. The result of petrophysical analysis is displayed below in Figure 4.3.

Table 4.1: Results determined for petrophysical analysis of Tajjal-02 well with two zones of interest identified, with their calculated attributes of porosity, water saturation, and hydrocarbon saturation being the following.

Serial Number	Calculation Parameters	Zone 1	Zone 2
1	Average Total Porosity = ϕ_{avg}	14.6%	7.8%
2	Average Effective Porosity in Percentage = ϕ_{avg}	11.72%	7.3%
3	Average Water Saturation in Percentage = S_{wavg}	75.14%	81.92%
4	Average Hydrocarbon Saturation in Percentage = S_{havg}	24.86%	18.08%

DRSM

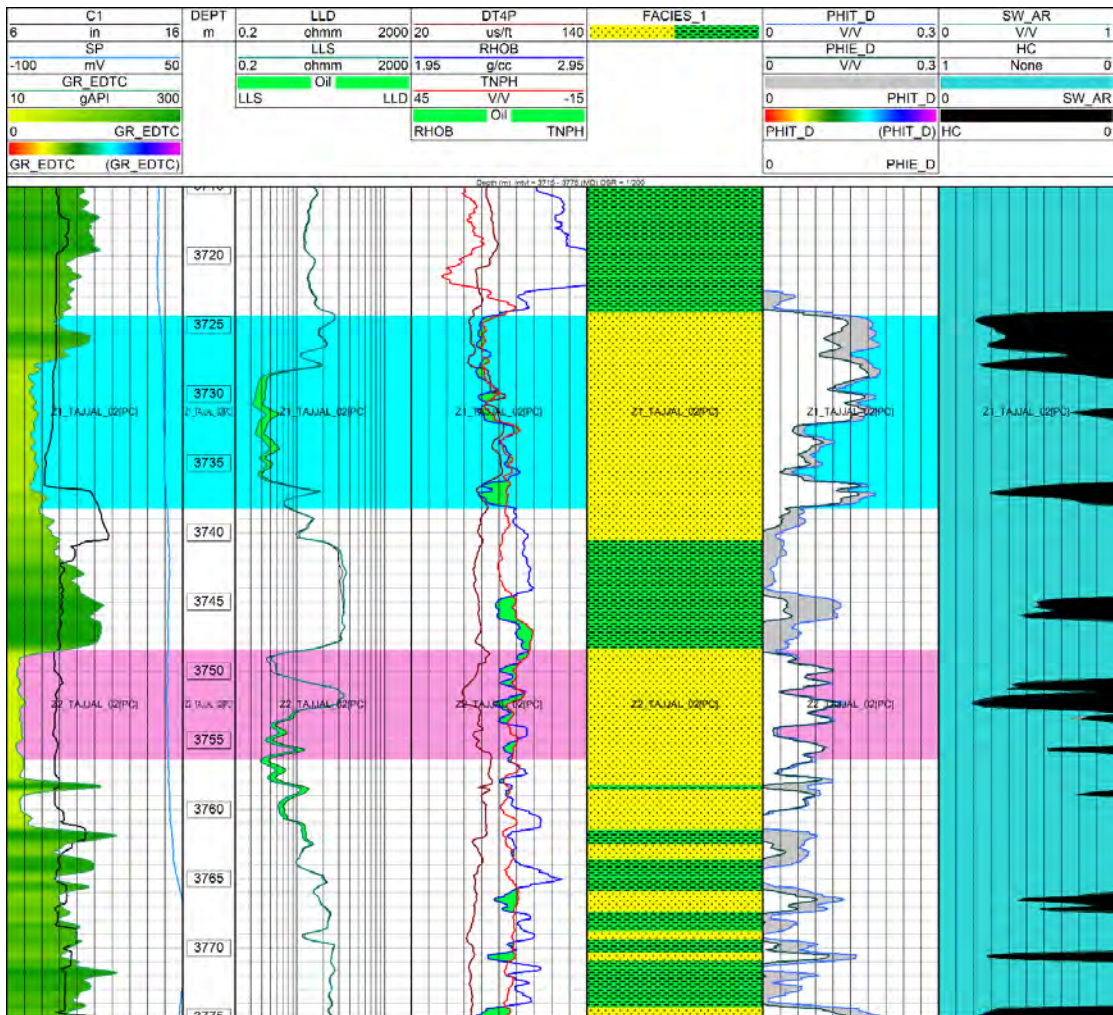


Figure 4.3: Interpreted section of Tajjal-02 well in the C Sands, where possible C sands presence can be confirmed with low volume of shale and high porosity, with two zones of interest identified with zone 1 have a net pay of 14m, while zone 2 having 7m.

CHAPTER 05

Seismic Inversion Analysis

5.1 Introduction

The efficient characterization of any reservoir requires the analysis of that reservoir using multiple geophysical tools. These tools can range from well based one-dimensional delineation of reservoir zones to the spatially applicable attributes that makes use of the properties of the seismic data, sometimes in combination of well data, to give important information regarding hydrocarbon signatures. Attributes such as inversion, lambda-rho, and mu-rho have been used to characterize the sands of Lower Goru.

The lambda and mu-rho attributes are generated from the impedance volumes acquired through inversion (Russell and Dommico, 1988). These volumes tell us about the presence of fluid and the lithology type respectively. To carry out the inversion, the following steps are carried out:

5.2 Wavelet Extraction

The seismic wavelet establishes a direct linkage between seismic data and the geologic rock properties while the accuracy in extraction of the wavelet directly influences the seismic inversion results (White, 1997). As convolution with earth reflectivity series is a difficult procedure, accurate wavelet extraction is required for effective use of inversion methods. Practically, the form of the source wavelet is impacted by both the time and depth, thus choosing the right type of wavelet is important. Geophysicists often prefer to derive wavelets from recorded seismic data over any theoretical wavelet (Cooke & Cant, 2010). This extracted wavelet has a combined effect of all the traces in the given data and therefore can generate an optimal synthetic seismogram. This generation requires the convolution of extracted wavelet with the reflectivity series and an additional noise component (Russell, 1988). Mathematically it can be shown as

$$s(t) = w(t) * r(t) + n(t), \quad (5.1)$$

where, $s(t)$ represents extracted wavelet, $r(t)$ is the reflection co-efficient (RC) series and $n(t)$ is the random noise. For this study, a statistical wavelet has

been extracted from seismic data with the wavelength of 0.02s, as shown in Figure 5.1. below.

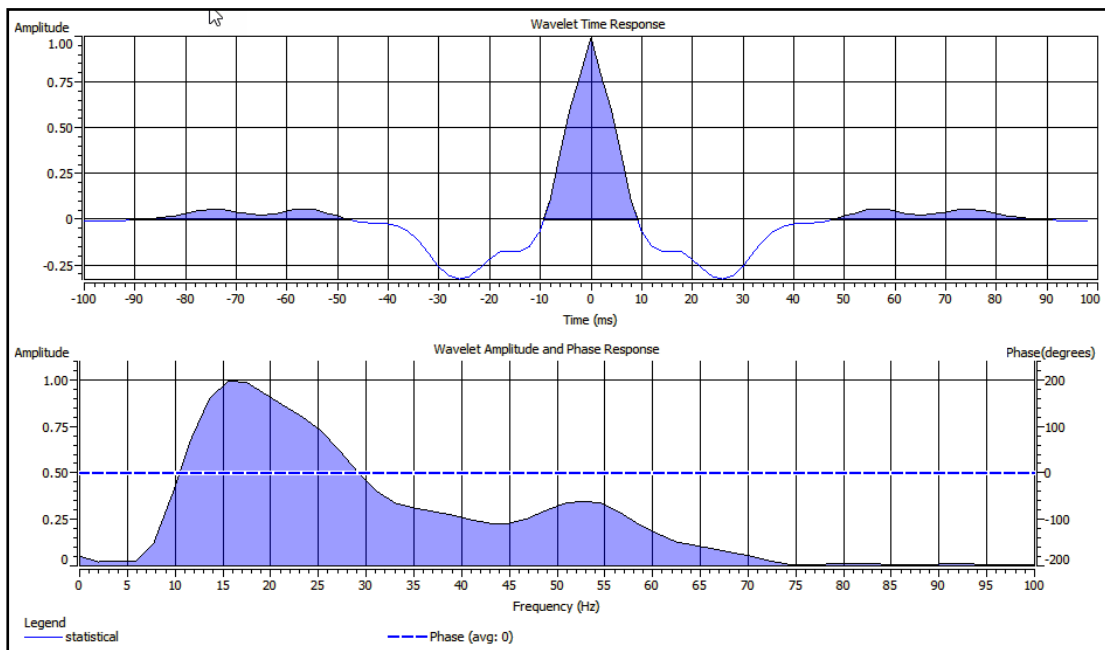


Figure 5.1. The statistical wavelet extracted from the seismic data with a wavelength of 0.02s.

5.3 Well-to-Seismic Tie

A well to seismic tie is compulsory at this stage as the recorded seismic data is prone to errors and tying it with a detailed well log ensures accuracy. Basically, it is a quality check taken as a safe measure to reduce uncertainty in further processes. Once a wavelet is extracted, correlation of well to seismic data is performed by following method: Synthetic trace is compared with the seismic trace within the vicinity of the well. Conformity among seismic and well reflectors is achieved by slight tweaks such as squeezing and stretching of time window. Correlation coefficient and RMS error are estimated between the adjusted well synthetic and real seismic trace. This is a repetitive procedure till the results occur within a suitable range. Correlation between well and seismic data at well TAJJAL-03 is 0.606. The correlation shows adequate matching of the extracted wavelet with recorded seismic data, hence making it suitable for inversion as shown in Figure 5.2.

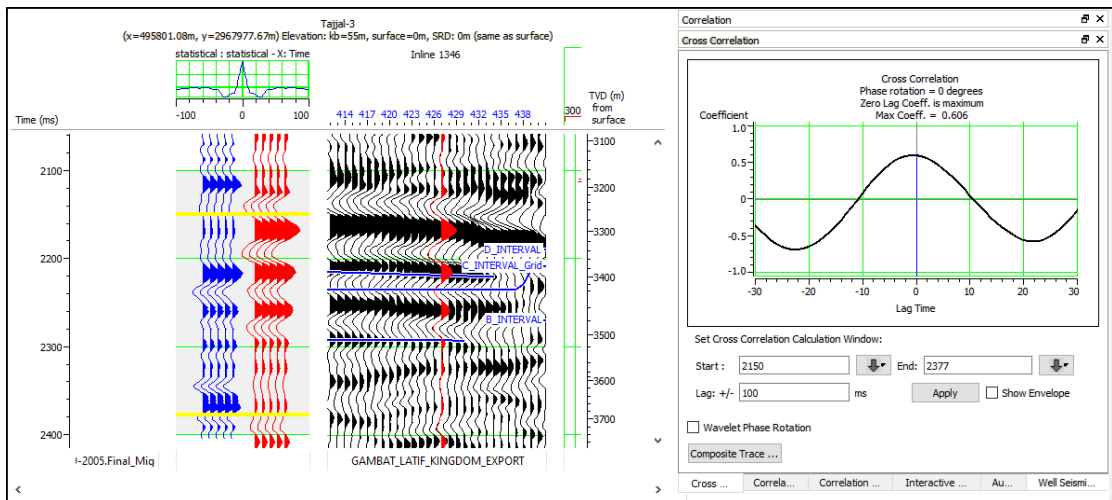


Figure 5.2: The correlation shows adequate matching of the extracted wavelet with recorded seismic data, hence making it suitable for inversion.

5.4 Initial Model/Low Frequency (LF) Model

Acoustic impedance has two types: Relative acoustic impedance and absolute acoustic impedance. Low frequency model is not essential in relative acoustic impedance as it is relative property of layers that is employed in qualitative interpretations. In absolute acoustic impedance, low frequency model is mandatory since it is an absolute layer property, and it is utilized for both qualitative and quantitative interpretation. Low frequency models are helpful in acquiring valuable information about changes in formations and it properly changes reflectivity into acoustic impedance (Cooke & Cant, 2010). In post stack seismic data, low frequency component is mostly removed in data processing, but seismic inversion needs low frequencies as they contain background information of data (Ray & Chopra, 2016). The low frequency model is generated using a low pass filter to regain the frequencies that have been lost in seismic data processing. A low frequency model is generated to recover the frequencies below 10 Hz and above 60 Hz as shown in Figure 5.3. This model is very helpful because it provides valuable information about gradual changes in C Sands Lower Goru Formation.

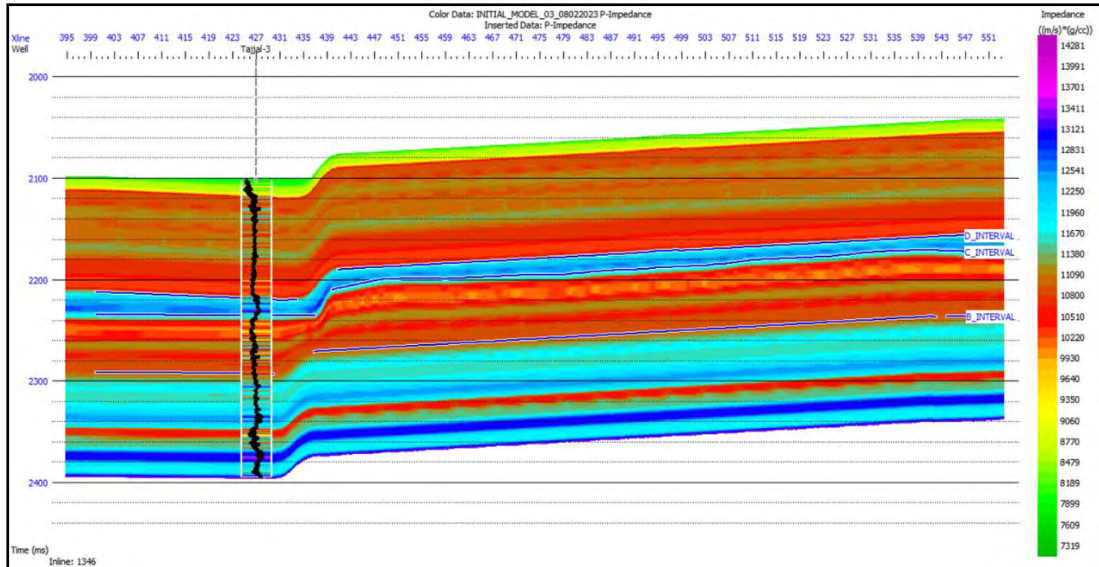


Figure 5.3: Cross section view of inline 1346 displaying the initial acoustic impedance values based on logs of Tajjal-03 created using Hampson and Russell (HRS) software.

5.5 Model-Based Inversion

Inversion has its origin characterized in the basic convolutional model, and by inverting that model, one can attain the reflectivity series, which can be further utilized to quantify layer properties. Model-based inversion is a broadband technique that builds an initial impedance model driven by well log data combined with the velocity information, and horizon information extracted from seismic (Toqeer et al., 2021). The initial acoustic impedance model is changed by comparing with the original seismic data, and the model is iterated and updated until misfit between seismic data and the synthetic seismogram that is obtained by convolving wavelet with the acoustic impedance model is removed. (Veeken, 2007; Simm and Bacon, 2014; Ashcroft, 2011). At first the well to seismic tie is performed for horizon marking, and well data is used to construct the initial earth model incorporating the low frequency trend, upon which a low frequency model is generated through well logs, and the horizons interpreted from seismic horizons. This is done to better characterize the stratigraphic features as more realistic and create a better geological model, to achieve the targeted realistic inverted impedance (Li and Zhao, 2014). A point of key concern to be mentioned is that the seismic data is bandlimited, thus low frequencies do not form part of the signal spectrum, and without these low frequencies the

prediction of reservoir properties is not unique and uncertain (Sams and Carter, 2017).

An acoustic impedance profile is generated through seismic inversion thus characterizing desired reservoir properties such as porosity, and for model-based inversion, the method starts by generating an initial geological model of earth and incorporating low frequency model from well log data, which further is iteratively checked in contrast the seismic data. Comparisons of the observed and calculated model are checked through forward modelling and the error is checked, and iterations occur till the uncertainty is removed, after which they stop.

To characterize the sands in C Sands and their potential, the model-based inversion was applied to the seismic volume. The section depicting the well Tajjal-03 and the seismic inline 1346 has been indicated in the Figure 5.5. The figure shows that the measured and estimated impedance logs have a 99% correlation between their synthetic seismograms.

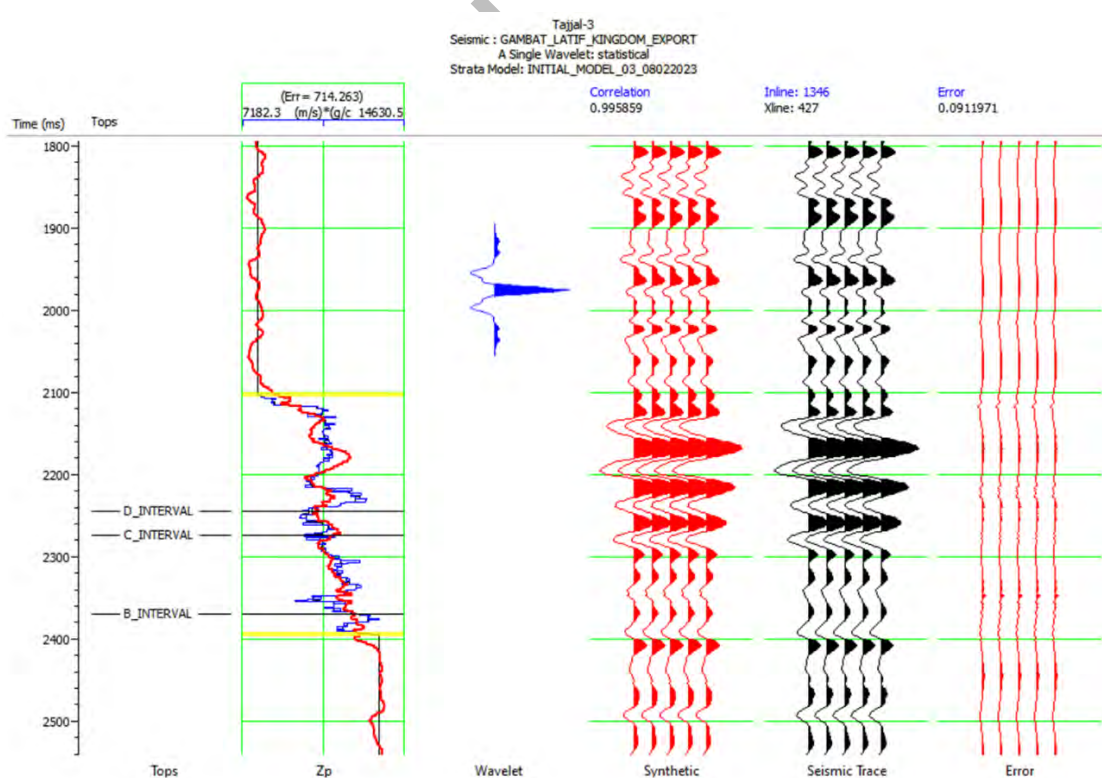


Figure 5.4: Statistical wavelet convolved with the extracted low frequency induced calculated geological model of the area for minimizing the uncertainty between calculated and observed models, with a 99% correlation was achieved using Hampson and Russel Software

The results from the Model-based inversion indicate that the C-Interval might have the potential hydrocarbon within the study area. (Figure 5.5).

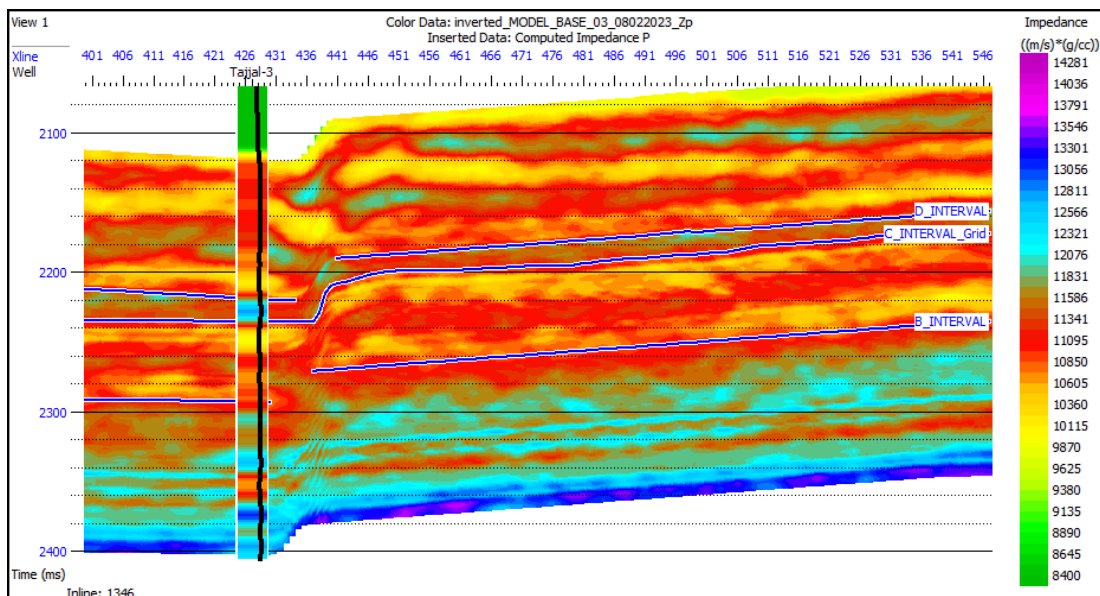


Figure 5.5: Cross section view of inline 1346 displaying the acoustic impedance contrast of lithologies with low impedance as sands, created using Hampson and Russell (HRS) software.

To identify any new prospect zone, the impedance was sliced from within the C-interval was taken. The results depict that the relatively low impedance values within the highlighted zone of interest might be a potential prospect zone (Figure 5.6). The impedance values within this zone are about $10000 (g/cm^3) * (m/s)$. This analysis can further be confirmed after applying the Lambda-rho and Mu-rho attributes.

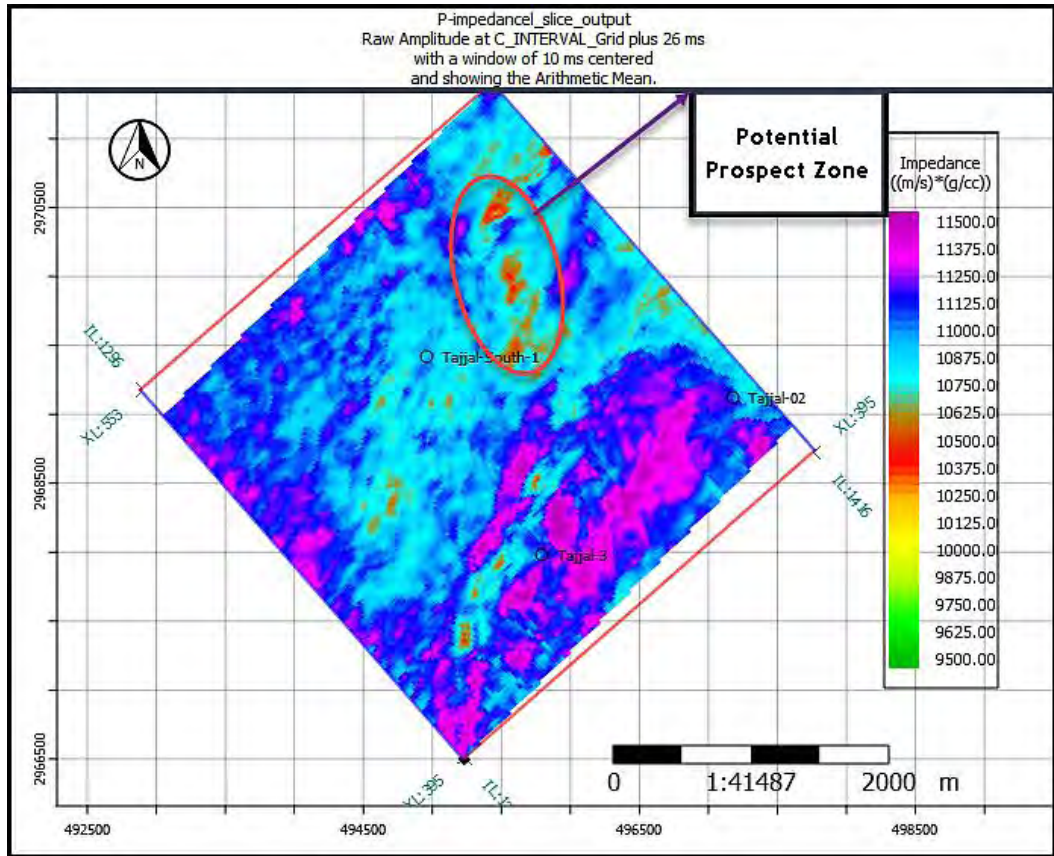


Figure 5.6: Acoustic impedance based on Model based inversion indicating potential prospect zone where the impedance values are relatively low.

5.3 Lambda-Mu-Rho Inverted Properties.

A more robust methodology is utilizing the inversion workflow in combination is by transforming the model-based inversion output volume into Lambda-rho and Mu-rho. The objective of this analysis is to determine the feasibility of segregating the reservoir facies and carrying out the imaging of the reservoir architecture with seismic attributes. Goodway et al., (1997) proposed the Lambda-Mu-Rho in which the Lambda and Mu parameters were introduced using Lamé's parameter (λ and μ) and density are prime components of the new simultaneous inversion approach. Equation 5.1 shows the relation between lambda-rho.

$$\lambda\rho = (\rho V_p)^2 - c(\rho V_p)^2 \quad (5.1)$$

where, V_p , V_s and ρ are P-wave velocity, S-wave velocity, and density, while c is a constant that is equal to 2. Russell et al., (2003) proposed that if the well log data is available than c for a given basin setting can be locally determined. The effect of fluid computation is influenced by the constant c ,

variable for different geological environments. Value of c falls within the range set by Dillon et al., (2003) that is applicable for both offshore and onshore. $\mu\rho$ is the square of S-wave impedance representing rigidity (rock matrix) given by the Equation 5.2.

$$\mu\rho = (\rho * Vs)^2 \quad (5.2)$$

The Lambda-Mu-Rho inversion is a powerful technique that can help in characterizing reservoir lithology and fluid distribution of sands in C Sands in Gambat-Latif block. Figure 5.7 displays the profile image of the lambda-rho attribute applied on the inline 1346 of Tajjal-03 well where the lambda-rho property is more susceptible to the pore fluids, with the maximum range having a purple color and value of 55 (GPa*g/cc), and a minimum represented by green color and a value of 22 (GPa*g/cc). Since more sensitivity to pore fluid, inversion results show a thick lithology of low impedance values with green and yellow color confirming the presence of gas saturated sands in the C Sands, and spatial distribution is given in time slice displayed in Figure 5.8.

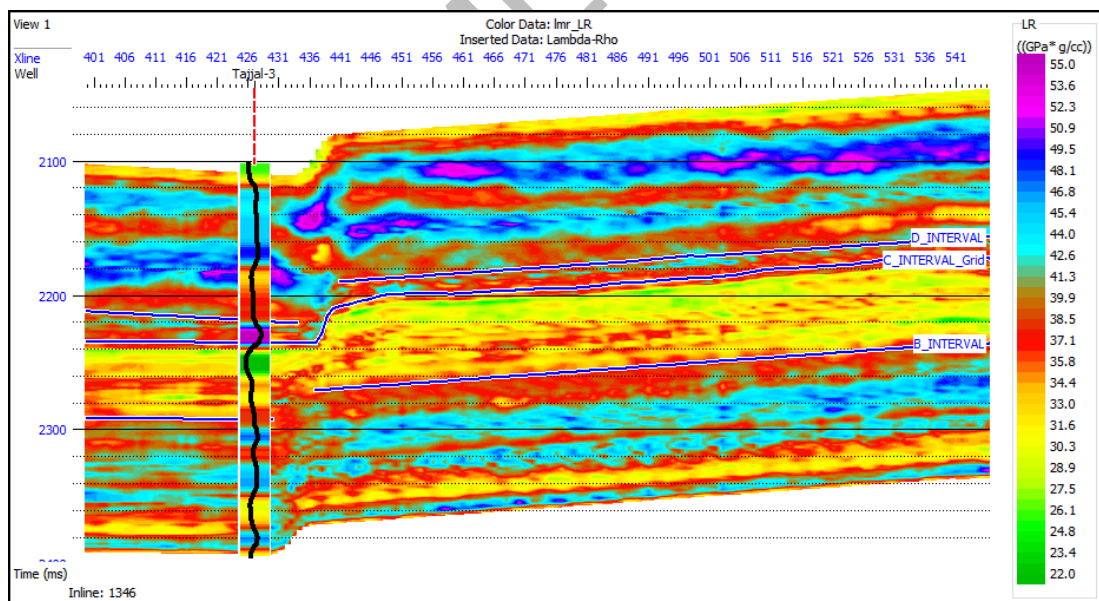


Figure 5.7: Spatial distribution of the acoustic impedance utilizing lambda-rho attributes, indicating similar pattern to model-based inversion spatial distribution but more refined to gas saturated reservoir sands, created using Hampson and Russell (HRS)

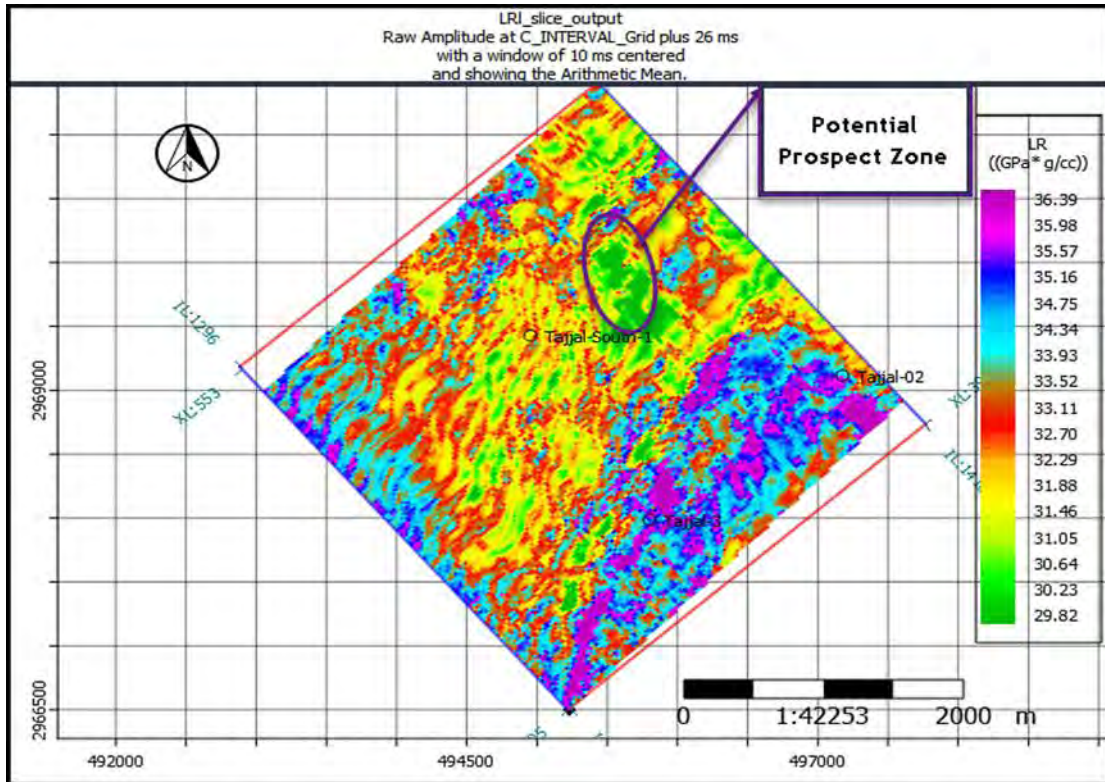


Figure 5.8: Lambda-rho attribute of the zone of interest in C-Interval indicating a potential prospect zone where the lambda-rho values are low, created using Hampson and Russel.

The Mu-rho property is sensitive to the rock matrix with a maximum to minimum range of 77 to 19 (GPa*g/cc), color varying from green (minimum) to purple (maximum). The cross section of the inline 1346 is displayed in Figure 5.9, where the rock matrix distinguished by mu-rho attribute is in a golden yellow color with a value range of 41.67 to 46.2 (GPa*g/cc), which is thicker in contrast to the sands identified by lambda-rho, but since it depends upon matrix rigidity, so pore fluids are more susceptible to response from lambda-rho. The spatial distribution of sands of C Sands is displayed in Figure 5.9.

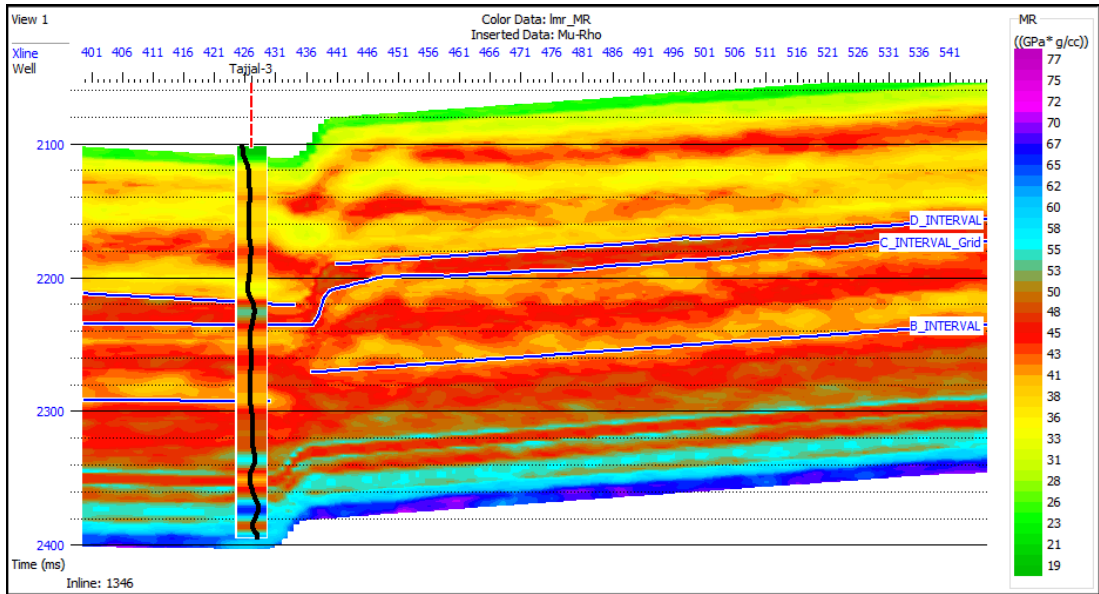


Figure 5.9: Mu-rho attribute applied to Tajjal-03 well, an attribute much sensitive to rock matrix indicates low acoustic impedance highlighted with green to yellow color as reservoir sand being porous sand bodies, created using Hampson and Russell (HRS)

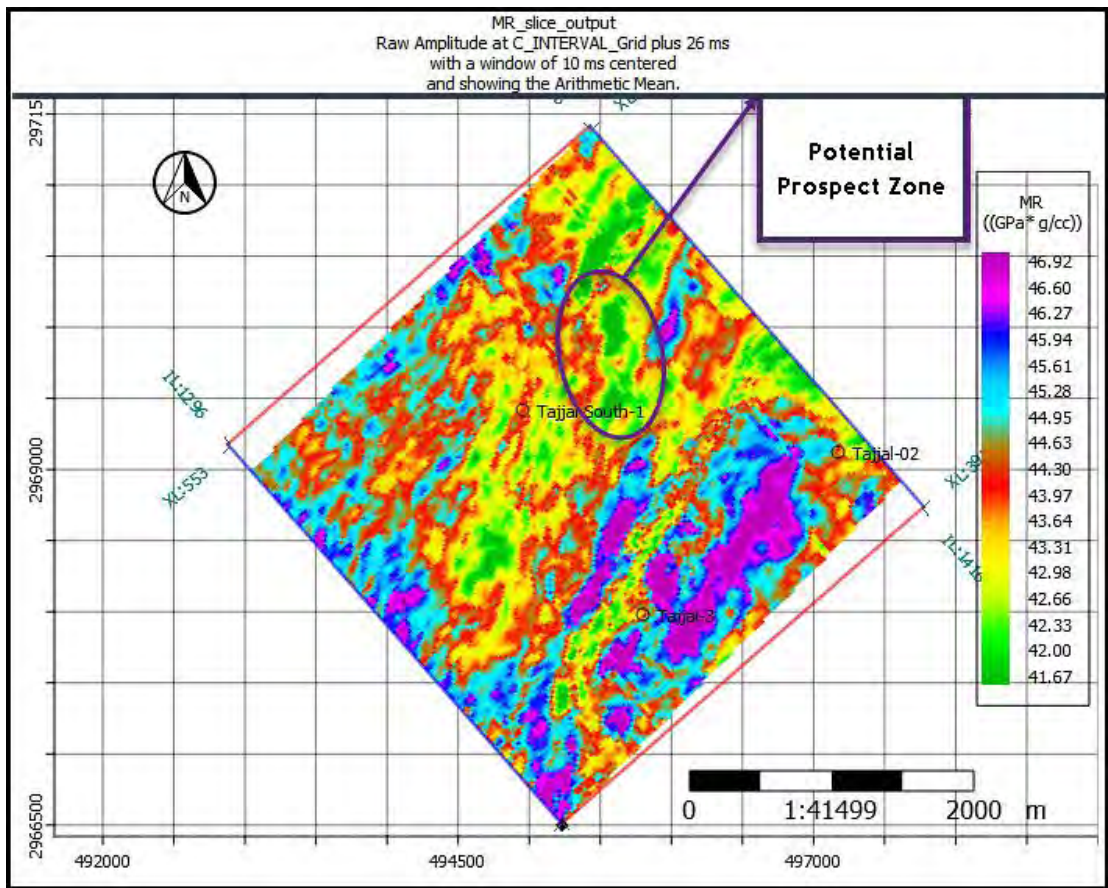


Figure 5.10: Mu-rho attribute slice of the zone of interest indicating that the identified potential prospect zone has moderate Mu-rho values. Using Hampson and Russel Software.

Chapter 6

Electrofacies and Sequence Stratigraphy

6.1 Introduction

The definition of "electrofacies," which was coined by Serra and Abbott in 1980, is "the set of log responses that characterize a bed and allow this to be distinguished from others." Given that log responses are evaluations of the physical characteristics of rocks, electrofacies are typically categorized into one or more lithofacies. Facies identification is crucial to petroleum exploration and reservoir characterization. In the past, facies were manually detected using graphical methods such cross-plotting from wire-line recordings and comparing their behavior to cores. To automate the process of facies identification, numerous mathematical models have recently been devised. These include approaches based on multivariate statistics and regression, such as Principal Component Analysis, Multivariate Analysis, Nonparametric Regression, Classification Trees, and methods based on Artificial Intelligence and Clustering.

6.2 Methodology

For this investigation, TAJJAL-02, worth of complete wireline logs accessible. To determine electrofacies, a sequence was built using the well log data of

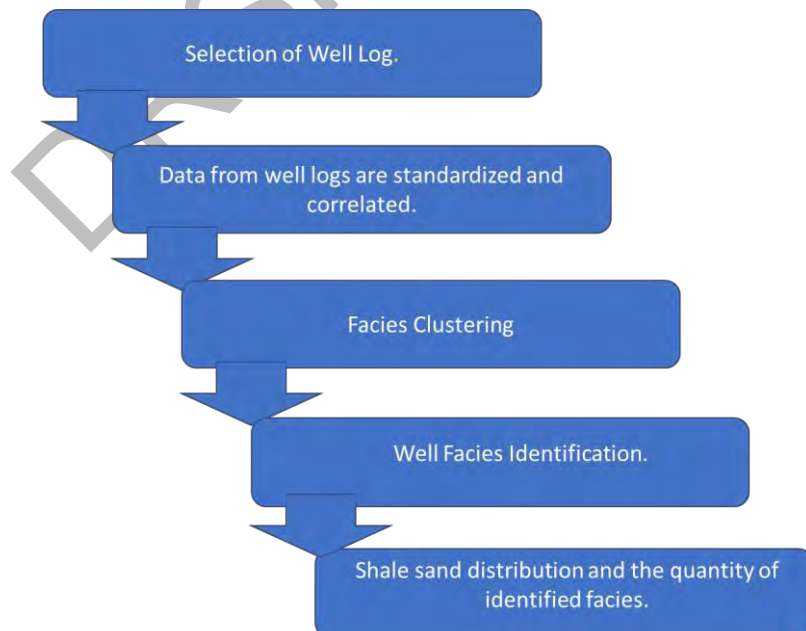


Figure 6.1: Flowchart showing the steps of electrofacies classification.

Techlog software is mostly used for interpreting well logs. If the well log data had recently been loaded by the software for better understanding. The subsequent stage involved choosing suitable logs. This inquiry makes use of gamma rays, resistivity, bulk densities, thermal neutron porosity, and sonic logs. These logs were used collectively since they yield the greatest results. In this instance, an IPSOM was generated by using the geology module to delineate the electrofacies zones. The electrofacies were determined using unsupervised techniques, and this fuzzy classification method was used. After that, electrofacies were used to determine the sand and shales distribution zone.

6.3 Electrofacies Classification

Gamma-ray and resistivity logs were run to categories the electrofacies. After choosing the logs, the well data was normalized to remove any changes brought on by different measuring methods. Facies clustering was performed, and the consistency of the logs was also checked.

With the use of PCA, clustering, and self-organizing maps, this categorization was carried out. Well logs were input into PCA in the form of matrix X $n \times p$, which has p variables and n objects (log curves). The following stage was correlating these variables and the matrix along the uncorrelated axes, then summarizing the results. The variance of each well log curve is the average squared variation of all its n values and can be estimated as:

$$V_i = \frac{1}{n-1} \sum_{m=1}^n (x_{im} - \bar{x}_i)^2 \quad (6.1)$$

Here,

- x_{im} represents the value of the i th variable in the object m .
- \bar{x}_i is the mean value of i .

Covariance is the measure of how much one variable influences the value of another. It is determined using the next equation.:

$$C_{ij} = \frac{1}{n-1} \sum_{m=1}^n (x_{im} - \bar{x}_i)(x_{jm} - \bar{x}_j) \quad (6.2)$$

Here,

- C_{ij} is the covariance of i and j variables.
- x_{im} and x_{jm} are the values of i and j variable in object m .
- \bar{x}_i and \bar{x}_j are the means of i and j .

The parameters covariance and variance are helpful for examining the differences in the dataset. Gamma ray and resistivity logs are chosen for PCA. These logs are then put into the Techlog program. The "techstat module" of this software uses pre-established algorithms to construct PCAs.

To clarify how PCA relates to the combination of various log curves, cross-plots for each unique log curve were created after PCAs. Additionally, PCA was cross plotted to perform cluster analysis and self-organizing maps in the Techlog IPSOM module for finding electrofacies, flowchart 6.1.

6.4 Fuzzy Classification Method

Cluster analysis and self-organizing maps are carried out via the fuzzy classification methodology in electrofacies classification by selecting unsupervised methods. Each node in fuzzy classification is given a probability-based random assignment to one of the groups.

Part 1: Each group is calculated using the barycenter method, weighted by the likelihood that each point belongs to the group:

$$\mu_k = \sum_{i=1}^n P_{ik}^{\frac{1}{QQ-1}} \cdot x_i \quad (6.3)$$

Here,

- P_{ik} is probability that the point i relate to the group k . The number of groups are defined by the class number parameter.
- μ_k is the barycenter of the group k .
- QQ is the weighting factor.

Part 2: New probabilities are calculated depending on the distance between each node and the barycenter of each group:

$$p_{nk} = \sum_{i=1}^{nbclasses} \left(\frac{ecart_{in}}{ecart_{kn}} \right)^{\frac{1}{Q-1}} \quad (6.4)$$

Here,

- p_{nk} : the probability that the point n belongs to the group k.
- $ecart_{kn} = \|x_n - \mu_k\|^2$: The distance between point n and the barycenter of group k.

Part 3: Convergence test: The algorithm checks for differences between the new and old probabilities:

- If yes, the new probabilities are used as input.
- If no, the new probabilities are the output of the model.

Output: The algorithm creates the probability. Each point's class is determined by its highest probability.

6.5 Tool for facies interpretation:

Log-curve form because the relationship between the log's shape and the rock successions' grain size, (Selley, 1978) thought of well-log curves as a fundamental tool for determining depositional facies. (Selley, 1979). There are five main types of log curves that are used to interpret the depositional environment. (Can't,1992) (models & 1992, n.d.). He also thought that analysis of core in relation to logs was a useful technique for understanding subsurface facies (as shown in Figure 6.2). The following are five types of log curves:

- Cylindrical shape.
- Funnel shape.
- Bell shape.
- Bow shape.
- Irregular shape.

6.5.1 Cylindrical shape:

Consistent gamma ray log measurements and sharp borders at the top and lower bounds indicate consistent lithology. The cylinder patterns, in other words, show homogeneous lithology.

6.5.2 Funnel Shape:

GR values can either decline upward from the maximum value of the log reading in trend or downward from maximum values, reflecting a decrease in shale content and generating an overall coarsening upward trend.

6.5.3 Bell shape:

Gamma ray values may rise upward from the minimum value of the log reading in trend, producing an upward trend, or they may rise significantly from minimum values, indicating a growth in shale content.

6.5.4 Bow shape:

This shape is the result of a gradually increasing cleaning sequence that deviates from its maximum value while maintaining a dirtying-up trend with the same grain size and no abrupt breaks. In other words, the trend is bow shape.

6.5.5 Irregular shape:

Gamma ray log motifs with irregular shapes are composed of varying gamma ray readings with high and low values over a relatively brief vertical well profile interval. These investigations revealed lithological variation in laminated layers, sand, and shale. PES addressing the link between sedimentology. (Nazeer et al., 2016; Selley, 1979)






Type of log motif shape	Cylindrical/box shape	Funnel shape	Bell shape	Symmetrical shape	Serrated/saw tooth shape
Sediment supply GR trend	Aggradation 	Progradation 	Retrogradation 	Petrograding & retrograding 	Aggrading 
Characteristic	Sharp top and base with consistent trend	Abrupt top with coarsening upward trend	Abrupt base with fining upward trend	Ideally rounded base and top	Irregular pattern/spikes of GR log
Grain size	Relative consistent lithology	Grain size increases	Grain size decreases	Cleaning upward trend change into dirtying up sequence from top	Inter-bedded shale's and sands
Depositional Environment	Aeolian (sand dunes), fluvial channels, carbonate shelf (thick carbonate), reef, submarine canyon fill, tidal sands, prograding delta distributaries	Crevasse splay, river mouth bar, delta front, shoreface, submarine fan lobe	Fluvial point bar, tidal point bar, deltaic distributaries, proximal deep sea, setting	Sandy offshore bar, transgressive shelf sands and mixed tidal flats environment	Fluvial flood plain, mixed tidal flat, debris flow and canyon fill

Figure 6.2: Facies correlation with a variety of other log shapes regarding the sedimentological relationship (Nazeer et al., 2016; Selley, 1979)

6.6 Results and Discussion

Utilizing the well logs from Tajjal-02, the electrofacies analysis was identified.

(i) **Geometrical shape:** GR readings are incredibly low and are falling.

(ii) **Funnel shape:** Low density and resistivity are indicated by intermediate GR values that are also decreasing upward.

(iii) **Bell shape:** The density and resistivity of the GR values are low to medium, and they are high with an ascending sequence.

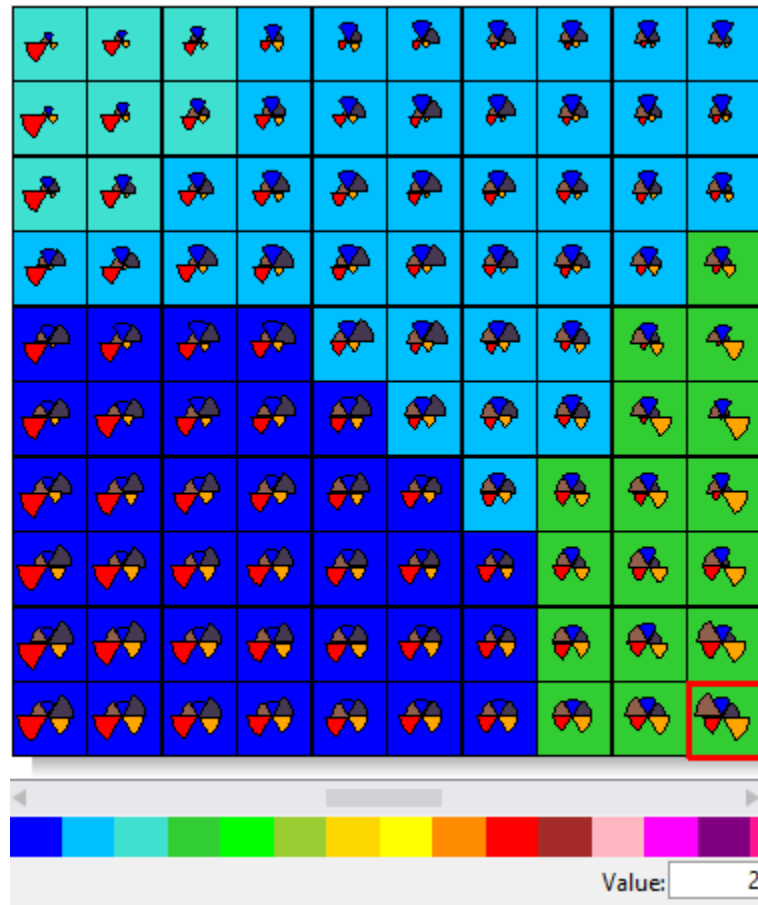


Figure 6.3: IPSOM electrofacies classification and self-organizing maps of Tadjal-02 based on Gamma ray (Dark grey color), Resistivity (Blue color), Thermal Neutron Porosity (Orange color), Bulk density (Brown color), and Sonic logs (Red color).

- In the above, 4 classifications are used.
- Each class shows percentage.
- Each color indicates different lithology and has quantitatively detected according to the percentage in the above figure.

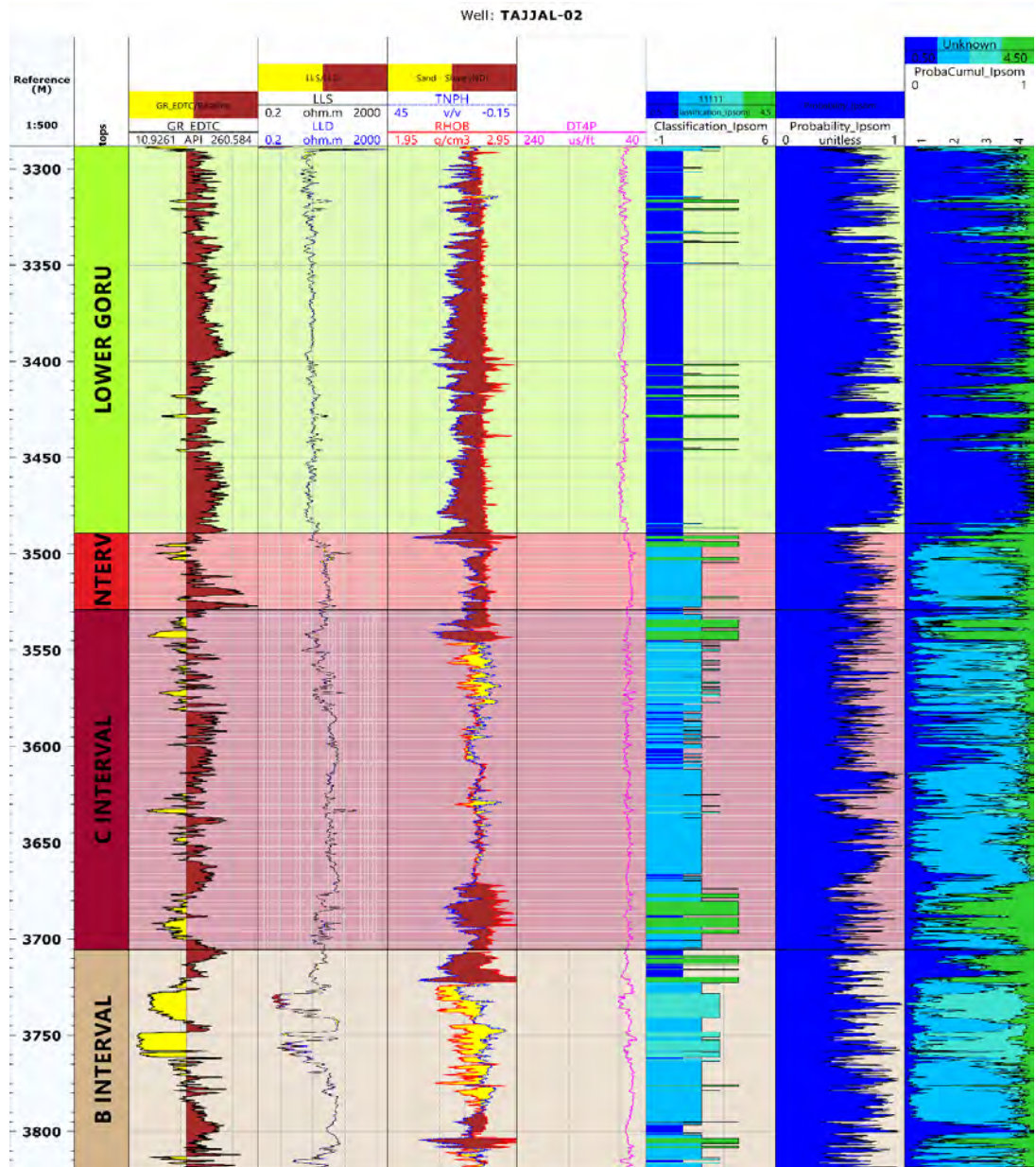


Figure.6.4: The electrofacies of well Tadjal-02 indicates four lithologies namely, shale (blue color), shaly sand (sky blue color), gas sand (cyan color), sandy shale (green color).

6.7 Zone of Interest

Table.6.1: The reservoir potential zones shown in the table below:

Well Name	Formation	Zone of interest(m)
TAJJAL-02	Lower Goru	B-Sands (3748 to 3761)
TAJJAL-02	Lower Goru	C-Sands (3530 to 3580)

The data's reduction in dimensions is PCA's main goal. After identifying the primary principal components, several facies were found using cluster analysis and self-organizing maps constructed using the Techlog program's IPSOM module. This classification was created on the grounds that the wireline log attributes lead to a rock that exhibits a distinctive convergence of physical traits. Each rock has a unique lithology, composition, degree of compaction, and pore fluid concentration. Analytical classification of a rock's electro facies results in an unpredictably large number of different electro facies; nevertheless, the number of pertinent electro facies is mostly reliant on the number of excellent log features utilized in their calculation.

Data from wells were used to classify the electro facies of the lower Goru zonation using self-organizing maps in Techlog's IPSOM module (Figure 6.3).

A self-organizing IPSOM map was created when the given values were entered into the software. Four different types of electro facies, namely shale, shaly sand, Gas Sand, and sandy Shale zones can be seen by using GR and LLD to study the map. Table 6.1. The reservoir zones are easy to recognize and indicate on this self-organizing map.

The investigation identifies four different electro facies that are Shale, Shaly Sand, Gas Sand (clean, porous sandstone), and Sandy Shale. First Navy Blue color signifies shale, Second Sky Blue color indicates Shaly Sand, Third Cyan color shows Gas Sand, and Fourth Green color indicates Sandy shale. (Figure 6.4).

6.8. Introduction to sequence stratigraphy:

Sequence stratigraphy is the study of sedimentary rock relationships within a chronostratigraphic or geologic-time framework and its basis is identification of strata surfaces, regional unconformities and their correlative conformities, and relationships among lithofacies and depositional environments, within this chronostratigraphic framework. While seismic stratigraphy is a geological approach to the stratigraphy interpretation of seismic data.

The seismic stratigraphy interpretation is marking of the depositional sequences and their subdivided system tracts on seismic data (Veeken, 2006). The delineation of depositional sequence boundaries is termed as the 'reflection termination mapping'

technique (Vail et al. 1977). Four major groups of systematic reflections are distinguished on seismic sections, sedimentary reflections, unconformities, artefacts, and non-sedimentary reflections (Veeken, 2006). These seismic reflections not only provide information about postdeposition structural deformation but also helpful to interpret geological time correlation; definition, thickness, and environment of genetic depositional units; paleo-bathymetry; burial history; unconformities and paleogeography and geological history. (Vail and Mitchum, 1977).

There are main three types of system tracts high stand, low stand and transgressive system tracts (HST, LST & TST respectively). Each system tract has its specific facies that differentiate one system tract to another. These facies can be analyzed by wireline logging (Rider, 1986) and by identifying different seismic reflection patterns on seismic sections (Veeken, 2006). Electro facies and electro sequence can be done by using well log data. GR and SP, the most widely used logs have different geometrical shapes to various facies such as bell, cylindrical or funnel shaped. But the composition of all logs called electro sequence gives precise result (Rider, 1986).

To achieve high resolution sequence stratigraphy different kinds of data such as core, cutting, biostratigraphy, and wireline data are used. Well data has high vertical resolution but there is no lateral information about the quality of reservoir rock. Simply seismic and well data are not enough to get high resolution facies. For this seismic inversion is best tool to imagine the distribution of the sequence facies throughout the reservoir because seismic data is converted to high quality acoustic impedance (AI) rather than amplitude (Atkins et al, 2001).

High resolution seismic data is always helpful to find out the stratigraphic traps such as carbonate traps, unconformities and entrapments in sandstone bodies such as buried stream channels, sandstone lenses, or sealed up dip terminations of sandstone onlapping against unconformities (Dobrin, 1977).

Proposed study area is Gambat-Latif area of Pakistan that is part of Lower Indus Basin and has significant importance stratigraphically and structural traps (Kazmi & Jan 1997).

6.8.1. Methodology

6.8.1.1. Wireline Logs Sequence Stratigraphy:

Different facies, depositional environment and sequence can be identified by using wireline logs. There is an example where sands are classified using GR/SP logs based on their geometrical shapes such as bell, cylindrical (blocky), and funnel Fig. 6.5. These shapes change accordingly to facies and depositional environment. GR log is an indicator of clay (shale) content, but by no means it always does. For example, a bell-shaped log where GR increases regularly upward from minimum value, indicates increasing shale contents. In funnel-shaped log the clay content decreases as GR decreases downward from high values (Fig. 6.5). It is also an indicator of grain size, where high GR shows fine grain and low GR indicates coarse grain. Point bars, channels, progradational, aggregational and transgressive facies environment can also be quantified using GR log as shown in Fig.6.6.

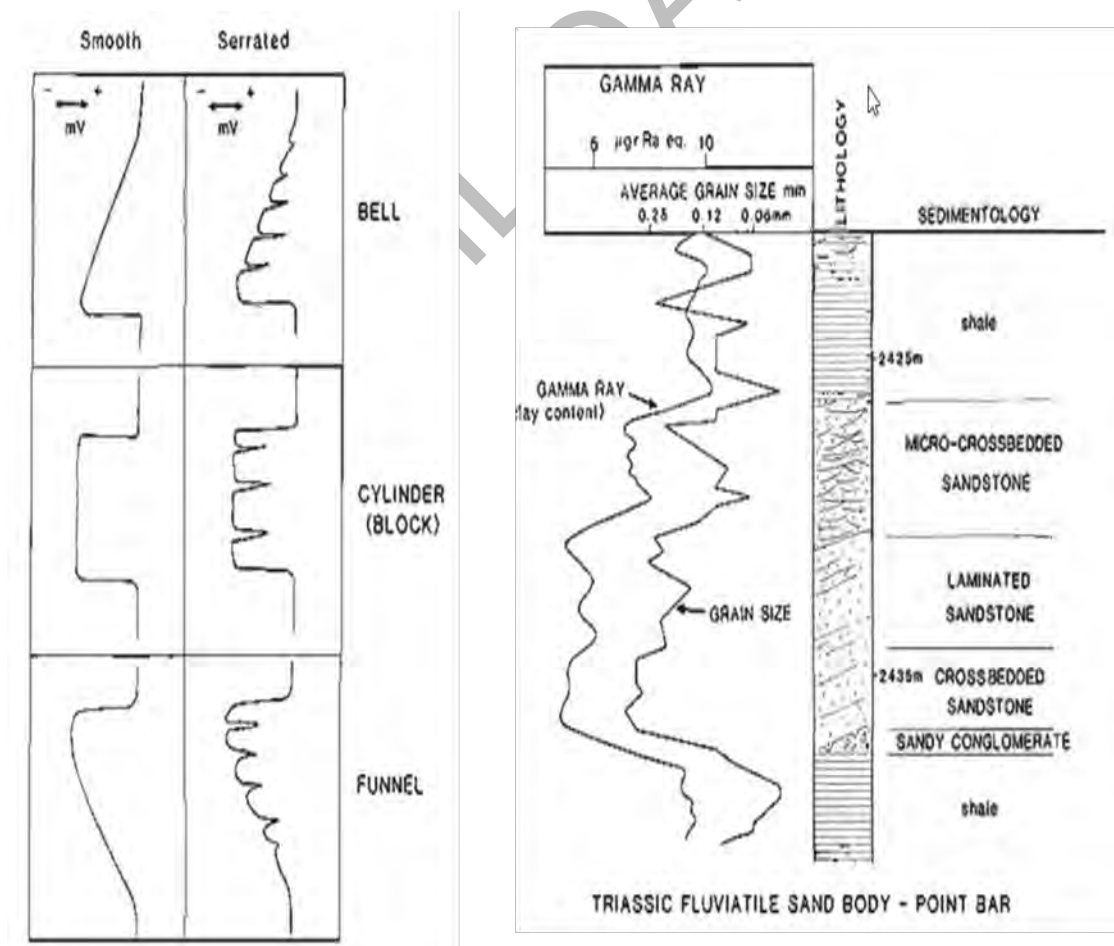


Figure 6.5: Shapes of GR logs (bell, cylindrical & funnel) show different lithology to bell shapes log (Serra & Sulpice, 1975; Rider, 1986).

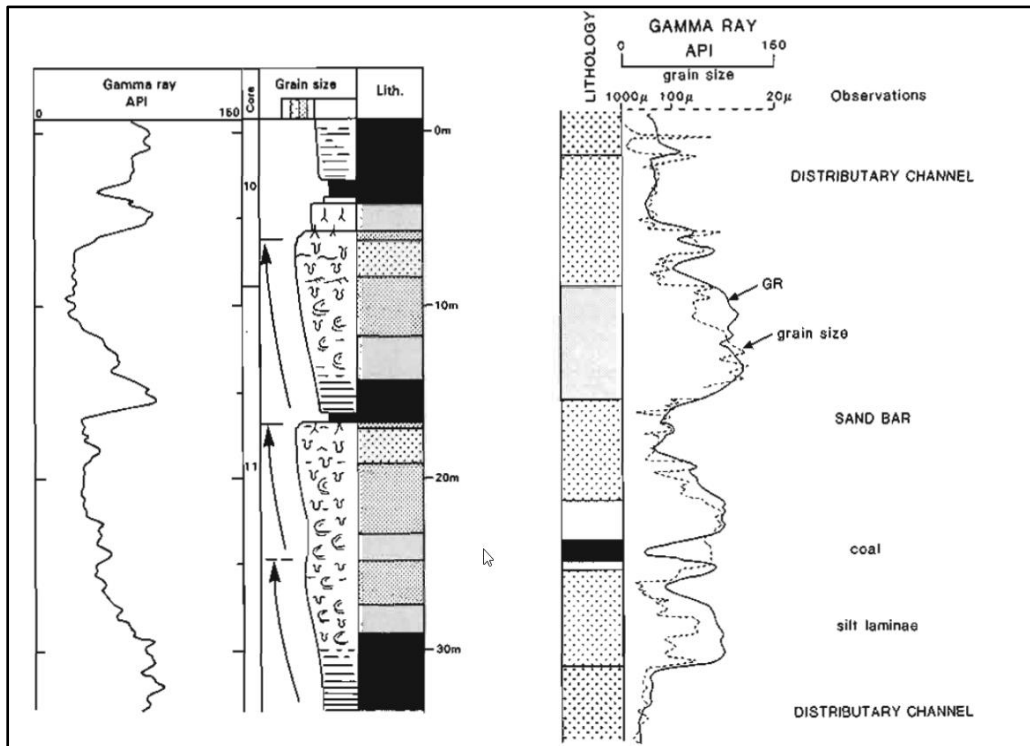


Figure 6.6: A funnel shape geometry of the log (left) coarsening upward sequence and grain size GR correlation (Rider, 1986).

DRSM

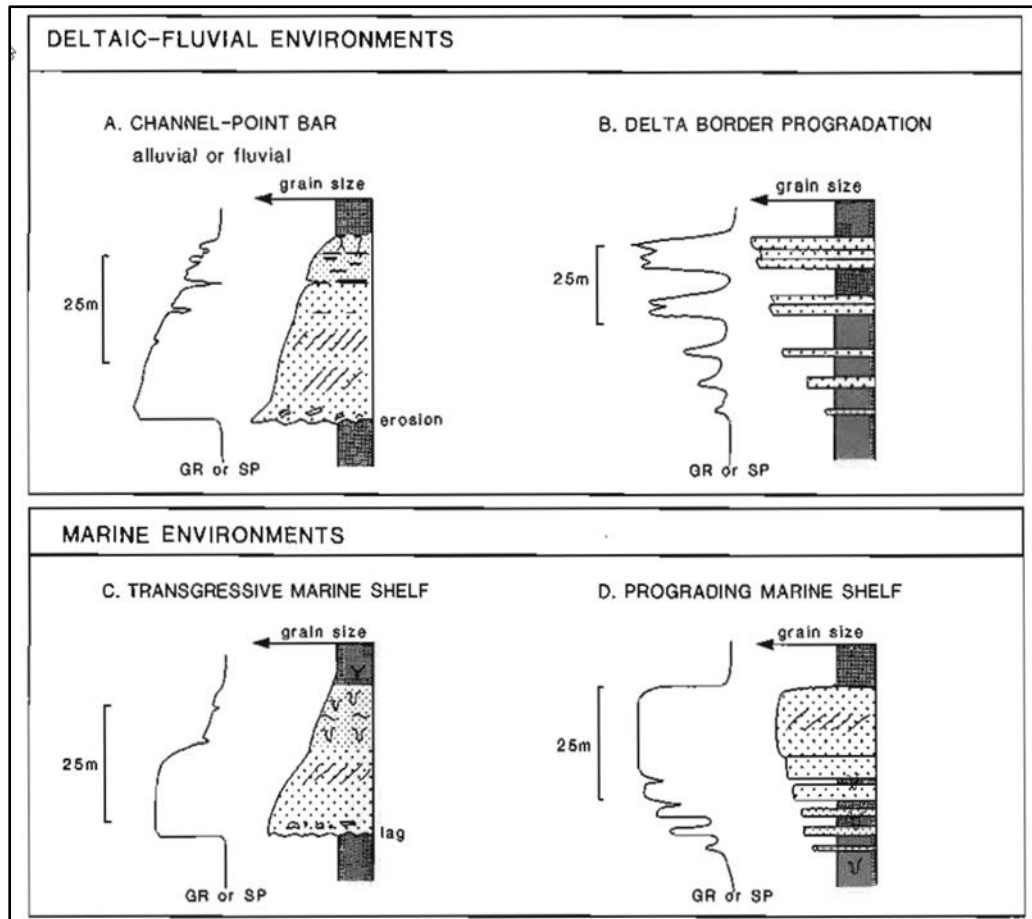


Figure 6.7: Another example of GR log that are showing point bars, channels, progradational, aggregational and transgressive facies environment and grain sizes of various facies (Serra, 1972; Parker, 1977; Galloway and Hobday, 1983).

6.8.2. Description of Sequences based on GR log.

Figure 6.8(a,b) describes different sedimentary sequences observed in a particular geological section and provides some information about the characteristics of these sequences. The first sequence discussed is an aggradational para sequence of the late high stand system tract (HST), which can be seen between the depths of 3512 to 3533 meters. This sequence is characterized by shale, in which the LLD and DT values are high. These conditions make it a potential prospect zone for hydrocarbon resources. Moving deeper, from 3533 to 3537 meters, a transgressive system tract (TST) is observed. TSTs occur when sea level rises, leading to a deposition of finer-grained sediments. This is followed by the Low stand system tract (LST), which can be seen from 3537 to 3548 meter, Finally, a progradational para-sequence observed from 3625 to 3646 meters, which consists of sedimentary facies that extend outward into a body of water, Different facies are observed within the log from 3645 to 3670 meters, consisting of progradational sedimentary facies. This provides a broad overview of the

different sedimentary sequences and facies present within the geological section interpreted based on GR log.

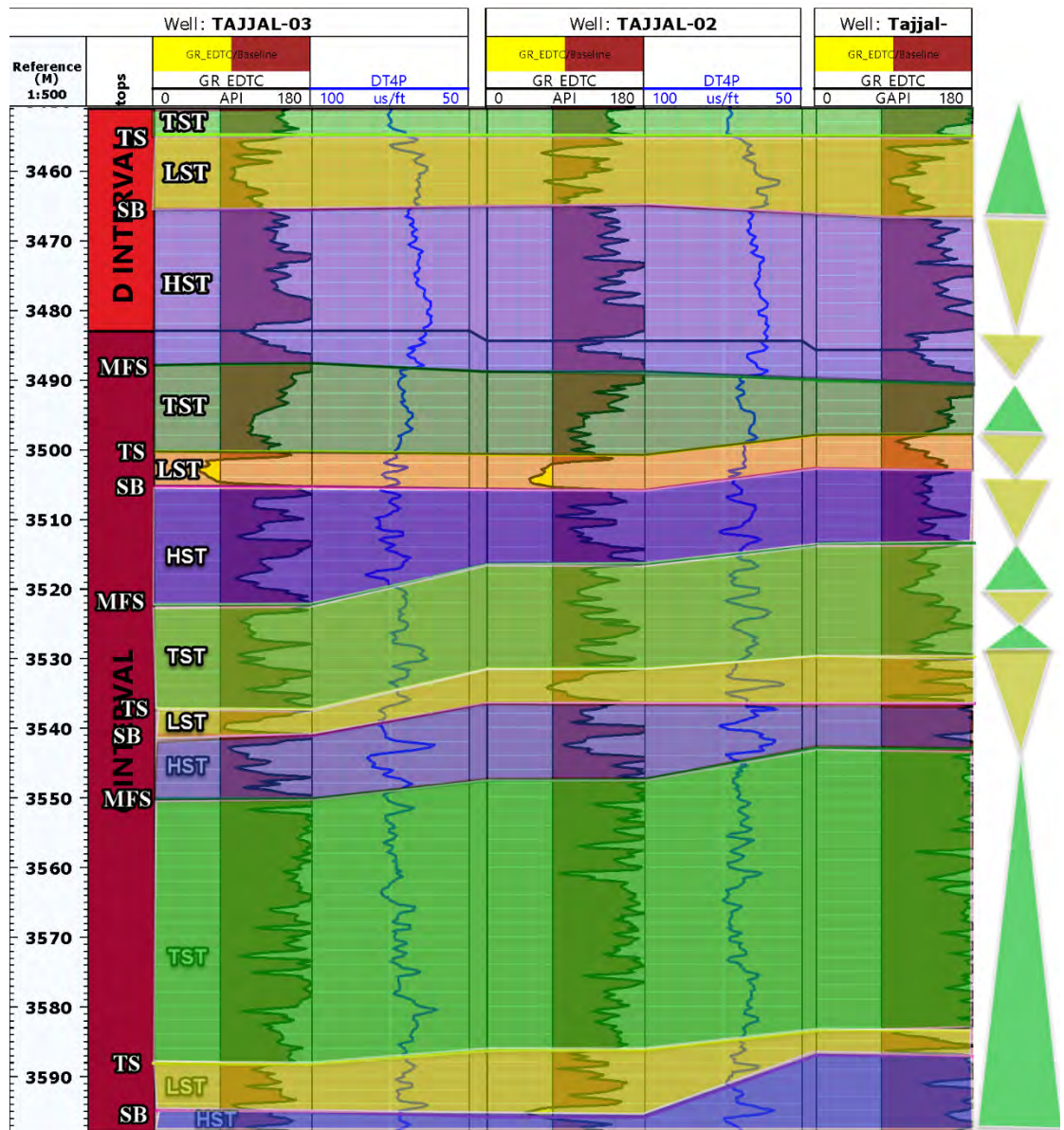


Figure 6.8(a): correlation of sequences in wells.

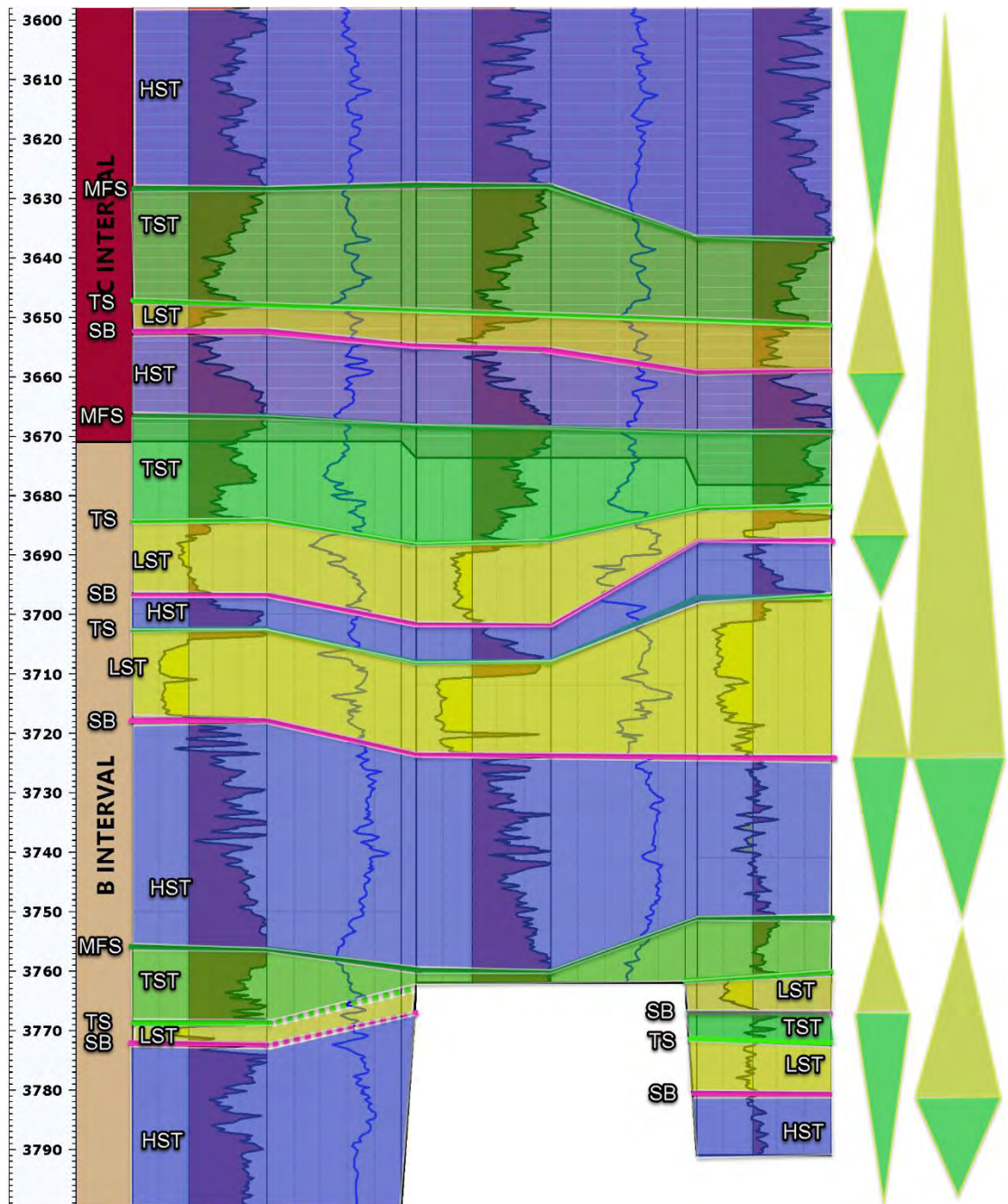


Figure 6.8(b): correlation of sequences in wells.

In figure 6.8, three wells are correlated, within these three wells, a total of seven sequences have been identified.

The first sequence spans from a depth of ... to 3773m and includes the observation of HST with shale deposition. In this sequence cycles repeated are LST, TST, and HST. The LST section (3773 to 3768) m is characterized by deposited sands that form a Transgressive surface (TS), above which TST begins. TST (3767 to 3755) m is marked by the deposition of shale, indicating the maximum flooding surface (MFS), after which

HST starts. HST (3754 to 3718) m ends at the sequence boundary, resulting in regression and progradational deposits.

The second sequence (3718 to 3697) m begins after the HST of sequence I, with LST (sands deposits), above which a Transgressive surface forms and HST starts. HST (3703 to 3897) m is characterized by the deposition of shale as the sea level regresses, and a progradational sequence forms, leading to the sequence boundary.

The third sequence (3697 to 3653) m is a repetition of the same cycle, with LST (3697 to 3685) m depositing sands above which a transgressive surface (TS) forms, followed by TST (3685 to 3666) m where sea level transgresses and retrogradational sediments deposit, marking maximum flooding surface (MFS), after which HST starts. HST (3666 to 3652) m is marked by the regression of sea level and progradational deposition, with shale decreasing and sand deposition marking the sequence boundary.

The fourth sequence (3652 to 3595) m follows the same cycles, beginning with LST (3652 to 3647)m depositing a thin bed of sand, above which sea level transgresses, and retrogradation starts depositing shale facies fining upward, forming a TS at a depth of 3647m, followed by TST (3647 to 3628) m where transgression takes place, and shale facies deposit, marking MFS at a depth of 3628m. HST (3628 to 3595) m is characterized by mostly shale deposition, with sea level fluctuations marking the sequence boundary.

The fifth sequence (3535 to 3542) m includes LST (3595 to 3587) m with increasing shale marking the TS, followed by TST (3587 to 3550) m with aggradation taking place, marking MFS at a depth of 3550m. HST (3550 to 3542) m shows a decrease in shale deposition.

The sixth sequence (3542 to 3505) m repeats the same cycles, beginning with LST (3542 to 3537) m depositing sand, followed by shale deposition marking TS at a depth of 3537m. TST (3537 to 3522) m is characterized by sea level fluctuations and marks MFS at a depth of 3522m, after which HST starts (3522 to 3505) m, with shale deposition and fluctuations in sea level.

The seventh sequence (3505 to 3965) m repeats all cycles, starting with LST (3505 to 3500) m depositing sand, marking TS,

CHAPTER 07

DISCUSSIONS AND CONCLUSIONS

7.1 Discussions

The study was focused on the characterization of the reservoir sands that are present in the mixed facies of the C Sands, in the Gambat-Latif block of the Lower Indus Basin, Pakistan. The study was characterized into stages from seismic structural interpretation and identification of the horizons in subsurface, after which petrophysical analysis were to determine presence of hydrocarbon footprint in the well data, on which the basis of reservoir characterization was laid out to better quantify the reservoir properties. The spatial distribution and further correlation were done utilizing inversion techniques to spatially map the reservoir quantitative properties using two different inversion techniques.

The study area is very potentially rich since there are major discoveries in surrounding blocks, of gas and oil. There have been different studies carried out by in the study area, but quantification of reservoir properties has been sparse, with most of the case scenarios run on isotropic fluid substitution, with changes observed in the cross plots on basis of gas and water saturation. The study was first conducted by identifying subsurface structure in the study block, that showed horst and graben structures, with the fault architecture being of synthetic faults, having no antithetic faults associated with fault trends in the NW-SE. The structure was much shallower in the western part of the study block, and got deeper in the east, which was observed in the values of time and depth contour maps.

After preliminary identification of the subsurface structure and depths associated with it, well data from the well Tajjal-02 underwent petrophysical evaluation, to locate zones of hydrocarbon accumulation in the study area. As the primary target for the study was the sands of C Sands, the petrophysical evaluation, yielded two zones of interest having hydrocarbon accumulation with Zone-1 yielding saturation of hydrocarbon of 24.69%, and Zone-2 showing hydrocarbon saturation of 17.86%.

Although petrophysical evaluation did confirm Tajjal-02 as being hydrocarbon bearing and sands of C Sands that could be coupled further with other sands of Lower Goru as high prospective targets, a further advanced step taken to correlate the petrophysical analysis with well data by quantifying the reservoir characteristics on basis of quantitative properties of impedance.

Characterization of reservoir properties was done using inversion techniques that combined both the well log data and the seismic data volume. Two different inversion techniques were applied to quantify the reservoir characteristics, in which model-based inversion yielded an almost similar geologic model as the observed and displayed areas of low acoustic impedance as porous sand facies, where further drop in the impedance indicated hydrocarbon presence in light green color. Unlike the model-based inversion that only provided an impedance contrast basis of quantification, the two different attributes namely lambda-rho and mu-rho were susceptible to different sets of information, in which lambda-rho which is more sensitive to the pore fluid presence in the porous media, while mu-rho better characterizes the rigidity of the rock matrix. The lambda-mu-rho inversion with the two attributes applied differently on the seismic inverted volume, where the lambda-rho confirmed low impedance values on inline 1346 using Tajjal-03 well and were spatially distributed on time slice, while the mu-rho attribute is also low on inline 1346 with combination of Tajjal-03 well and then spatially spread out on the data set.

Electrofacies are identified on the well log data. Four facies are identified as gas sand, shaly sand, sandy shale, and shale. Gas sand has been observed in the well with the help of electro facies. Sequence stratigraphy is applied on well data and sequences are identified which are, based on the description of the sedimentary sequences and sub-zones in this geological section, some potential findings can be inferred suggesting that the geological section contains a diverse range sequences and sub-zones, including retrogradational, and progradational para sequences, as well as the HST, TST, and LST. The HST is characterized by coarse-grained deposition.

In aggradational para sequences, the TST is associated with a rise in sea level and finer-grained sediments. The LST occurs when sea level falls, and coarser-grained sediments are deposited. These findings provide valuable information for understanding the geological history and potential resource opportunities of the studied area the aggradational para sequence of HST, which consists of coarse-grained deposits and shale with low sea level delta. The presence of progradational sedimentary facies in LST and TST may indicate a change in sediment supply or sea level fluctuations, which could have implications for the interpretation of the geological history of the region. Overall, the sedimentary sequences and facies observed in this geological section provide important information for understanding the geological history and potential resource prospects of the area.

DRSML QAU

References

- Abbasi, S., Kalwar, Z., and Solangi, S. 2016. Study of structural styles and hydrocarbon potential of Rajan Pur Area, Middle Indus Basin, Pakistan; *BUJES 1*. 36-41.
- Ahmed, R., All, S. M., & Ahmad, J. (1994). Review of petroleum occurrence and prospects of Pakistan with special reference to adjoining Basins of India, Afghanistan, and Iran. *Pakistan Journal of Hydrocarbon Research*, 6(1 & 2), 7-18.
- Alam MSM, Wasimuddin M, Ahmad SSM (2002) Zaur structure, a complex trap in poor seismic data area, BP Pakistan Exploration and Production Inc. PAPG/SPE ATC conference. Islamabad, Pakistan, pp 1–3
- Ali, A., Alves, T. M., Saad, F. A., Ullah, M., Toqeer, M., and Hussain, M. 2018. Resource potential of gas reservoirs in South Pakistan and adjacent Indian subcontinent revealed by post-stack inversion techniques: *J. Nat. Gas Sci. Eng.* 49 41–55.
- Amir, A., Kenyon, N. H. N. H., Cramp, A., & Kidd, R. B. (1996). Morphology of Channel Levee Systems on the Indus Deep-Sea Fan, Arabian Sea. *Pakistan Journal of Hydrocarbon Research*, 8, 43-53.
- Ashcroft, W. 2011. *A Petroleum Geologist's Guide to Seismic Reflection*, Wiley–Blackwell.
- Ashraf, U., Zhu, P., Yasin, Q., Anees, A., Imraz, M., Mangi, H. N., & Shakeel, S. (2019). Classification of reservoir facies using well log and 3D seismic attributes for prospect evaluation and field development: A case study of Sawan gas field, Pakistan. *Journal of Petroleum Science and Engineering*, 175, 338-351.
- Asquith, G. B., Krygowski, D., & Gibson, C. R. (2004). *Basic well log analysis* (Vol.16). Tulsa, OK: American association of petroleum geologists.
- Atkins, D. R., Wilson, M., & Sams, M. S. (2001, June). Sequence Stratigraphy and Seismic Impedance-A New Approach to Reservoir Characterisation. In 63rd EAGE Conference & Exhibition.

Atkins, D., Wilson, M., & Sams, M. (2001). Sequence Stratigraphy and Seismic Impedance-A New Approach to Reservoir Characterisation in 63rd Mtg. Eur. Assn. Geosocial. Eng., Expanded Abstracts, Session: F-31.

Avseth, P., Mukerji, T., and Mavko, G. 2005. Quantitative seismic interpretation: Applying rock physics tools to reduce interpretation risk, Cambridge University Press, <https://doi.org/10.1017/CBO9780511600074>.

Aziz, M. Z., and Khan, M. R. 2003. A review of Infra-Cambrian source rock potential in Eastern Sindh, an analogue to Huqf Group of Oman. Infra-Cambrian play of Eastern Sindh, Pakistan.

Bacon, M., Simm, R., and Redshaw, T. 2007. 3-D seismic interpretation, Cambridge University Press, <https://doi.org/10.1017/CBO9780511802416>.

Biswas, S. K. (1982). Rift basins in western margin of India and their hydrocarbon prospects with special reference to Kutch basin. AAPG Bulletin, 66(10), 1497-1513.

Dobrin, M. B. (1977). Seismic Exploration for Stratigraphic Traps: Section 2. Application of Seismic Reflection Configuration to Stratigraphic Interpretation.

Bjorlykke, K., 2010 Petroleum Geoscience: From Sedimentary Environments to Rock Physics, Springer.

Bosch, M., Carvajal, C., Rodrigues, J., Torres, A., Aldana, M., and Sierra, J. 2009. Petrophysical seismic inversion conditioned to well-log data: Methods and application to a gas reservoir; Geophysics 74 O1–O15, <https://doi.org/10.1190/1.3043796>.

Bosch, M., Mukerji, T., and Gonzalez, E. F. 2010. Seismic inversion for reservoir properties combining statistical rock physics and geostatistics: A review; Geophysics 75 75A165, <https://doi.org/10.1190/1.3478209>.

Chen, Q., and Sidney, S. 1997. Seismic attribute technology for reservoir forecasting and monitoring; Lead Edge 16 445–448, <https://doi.org/10.1190/1.1437657>.

Chopra, S., and Marfurt, K. J. 2007. Seismic attributes for prospect identification and reservoir characterization: Geophysics. Dev. Ser. 11465, <https://doi.org/10.1190/1.9781560801900>.

Delaplanché, J., Lafet, Y., and Sineriz, B. 1982. Seismic reflection applied to sedimentology and gas discovery in the Gulf of Cadiz: *Geophys. Prospect.* 30 1–24.

Dillon, L., Schwedersky, G., Vasquez, G., Velloso, R., and Nunes, C. (2003). A multiscale DHI elastic attributes evaluation: *The Leading Edge*, 22, 1024-1029.

Dobrin, M.B. and Savit, C.H. (1988) *Introduction to Geophysical Prospecting*. 4th Edition, McGraw-Hill, New York, 867p

Euzen, T., Delamaide, E., Feuchtwanger, T., & Kingsmith, K. D. (2010, October). Well log cluster analysis: an innovative tool for unconventional exploration. In *Canadian unconventional resources and international petroleum conference*. OnePetro.

Galloway, W. E. (1989). Genetic stratigraphic sequences in basin analysis I: architecture and genesis of flooding-surface bounded depositional units. *AAPG bulletin*, 73(2), 125142.

Galloway, W. E., & Hobday, D. K. (1983). *Terrigenous clastic depositional systems: applications to petroleum, coal, and uranium exploration*. Springer-Verlag, New York.

Goodway, B., Chen, T., and Downtown, J. 1997. Improved AVO fluid detection and lithology discrimination using Lamé petrophysical parameters; $\lambda\rho$, $\mu\rho$ & $\lambda\rho/\mu\rho$ fluid stack, from P- and S inversions: Presented on 67th Annual international Meeting, SEG Expanded Abstracts, pp. 183–186.

Grana, D. and Dvorkin, J. 2011. The link between seismic inversion, rock physics, and geostatistical simulations in seismic reservoir characterization studies; *Lead Edge* 30 54–61, <https://doi.org/10.1190/1.3535433>.

Han, D. H., & Batzle, M. L. (2004). Gassmann's equation and fluid saturation effects on seismic velocities. *Geophysics* 69, no. 2 (2004): 398-405.

Hearts, J. R., Nelson, P. H., and Paillet, F. L. 2002. *Well Logging for Physical Properties: A Handbook for Geophysicists, Geologists and Engineers*, 2nd edn, John Wiley & Sons, Chichester.

Kadri, I. B. (1995). *petroleum geology of Pakistan*, Karachi, Feroz sons (pvt) ltd.

Kadri, I. B. (1995). Petroleum geology of Pakistan (p. 273). Karachi: Pakistan Petroleum Limited

Kazmi AH, Sneer LW (1989) Geology of world emerald deposits: a brief review. Van Nostrand Reinhold publishers, The Netherland.

Kazmi, A. H., & Jan, M. Q. (1997). Geology and tectonics of Pakistan. Graphic publishers.

Kazmi, A. H., & Rana, R. A. (1982). Tectonic Map of Pakistan, 1:1000000. Geology Survey of Pakistan, Quetta, Pakistan.

Kazmi, A. H., Abbasi, I. A. (2008). Stratigraphy & Historical Geology of Pakistan, Department & National Centre of Excellence in Geology.

Kazmi, A.H & Jan, M.Q, (1997), Geology and tectonics of Pakistan, Graphic publisher, Karachi, Pakistan.

Khalid, P., Akhtar, S., & Khurram, S. (2020). Reservoir characterization and multiscale heterogeneity analysis of Cretaceous reservoir in Punjab platform of Middle Indus Basin, Pakistan. *Arabian Journal for Science and Engineering*, 45, 4871-4890.

Kim, H. J. (2008). Common factor analysis versus principal component analysis: choice for symptom cluster research. *Asian nursing research*, 2(1), 17-24.

King, D. E. 1990. Incorporating geological data in well log interpretation; In: Geological Applications of Wireline Logs, pp. 45–55, <https://doi.org/10.1144/gsl.sp.1990.048.01.06>.

Kingston, D. R., Dishroon, C. P., & Williams, P. A. (1983). Hydrocarbon plays and global basin classification. *AAPG bulletin*, 67(12),2194-2198.

Landa, J. L., Horne, R. N., Kamal, M. M., and Jenkins, C. D. 2000. Reservoir characterization constrained to well-test data: A field example SPE Reserv. Eval. Eng. 3 325–334, <https://doi.org/10.2118/65429-PA>.

Li, M., and Zhao, Y. 2014. Chapter 6 – Seismic inversion techniques. In: Geophysical Exploration Technology Applications in Lithological and Stratigraphic Reservoirs, Elsevier, Oxford, pp. 133–198, <https://doi.org/10.1016/B978-0-12-410436-5.00006-X>.

Li, Y., Lin, S., Wang, H., & Luo, D. (2017). Depositional setting analysis using seismic sedimentology: Example from the Paleogene Lishagang sequence in the Fushan depression, South China Sea. *Geodesy and Geodynamics*, 8(5), 347-355.

Lindseth, R. O. 1979. Synthetic sonic logs – a process for stratigraphic interpretation; *Geophysics* 44-3, <https://doi.org/10.1190/1.1440922>.

Liner, C. 2016. Elements of 3D seismology, investigations in geophysics; Society of Exploration Geophysicists, <https://doi.org/10.1190/1.9781560803386>.

Mavko G, Mukerji T and Dvorkin J 2009 *The Rock Physics Handbook* 2nd edn (New York: Cambridge University Press).

Mitchum Jr, R. M., Vail, P. R., & Thompson III, S. (1977). Seismic stratigraphy and global changes of sea level: Part 2. The depositional sequence as a basic unit for stratigraphic analysis: Section 2. Application of seismic reflection configuration to stratigraphic interpretation.

Nazeer, A., Abbasi, S. A., & Solangi, S. H. (2016). Sedimentary facies interpretation of Gamma Ray (GR) log as basic well logs in Central and Lower Indus Basin of Pakistan. *Geodesy and Geodynamics*, 7(6), 432-443.

Onajite, E. (2013). Seismic data analysis techniques in hydrocarbon exploration. Elsevier.

Parker, J. R. (1977). Deep-sea sands. *Developments in petroleum geology*, 1, 225-242.

Pomerol, C., Y. Lagabrielle and M. Renard, 2005, *Elements de Geologie*. Dunod, Paris, 762p.

Raza, H. A., Ahmed, R., Ali, S. M., Sheikh, A. M., & Shafique, N. A. (1989). Exploration performance in sedimentary zones of Pakistan. *Pakistan Journal of Hydrocarbon Research*. v.1/1. p.1-7.

Raza, H. A., Ali, S. M., & Ahmed, R. (1990). Petroleum geology of Kirthar sub-basin and part of Kutch Basin. *Pakistan Journal of Hydrocarbon Research*, 2(1), 27-73.

Rider, M. H. (1996). *The Geological Interpretation of Well Logs*; John Wiley and Sons, New York.

Russell, B. H., Hedlin, K., Hilterman, F. J., and Lines, L. R. (2003). Fluid property discrimination with AVO: A Biot-Gassmann perspective: *Geophysics*, 68. 29-39.

Russell, B., and Dommico, S. 1988. Introduction to seismic inversion methods, SEG.

Sams, M., and Carter, D. 2017. Stuck between a rock and a reflection: A tutorial on lowfrequency models for seismic inversion; *Interpretation* 5 B17–B27.

Sangree, J. B., & Widmier, J. M. (1977). Seismic stratigraphy and global changes of sea level: Part 9. Seismic interpretation of clastic depositional facies: Section 2. Application of seismic reflection configuration to stratigraphic interpretation.

Schlumberger, L. I. (1989) Principles and Application: Schlumberger Wireline and Testin. *Houston, Texas*, 21-89.

Seemann, W., Allmed, W. & Alam, S., 1988. "Source Rock Potential of Rock Samples from Kirthar Range", Hydrocarbon Development Institute of Pakistan Lab. Report 1988/1.

Selley, R. C. (1979). Concepts and methods of subsurface facies analysis.

Serra, O. (1972). Diagraphies et stratigraphie. *Memoirs BRGM*, 77.

Serra, O. and H. T. Abbott (1980): The contribution of logging data to sedimentology and stratigraphic, SPE 9270, 55th Annual Fall Technical Conference and Exhibition, Dallas, Texas, 19p

Serra, O., & Sulpice, L. (1975, January). Sedimentological analysis of shale-sand series from well logs. In SPWLA 16th Annual Logging Symposium. Society of Petrophysicists and Well-Log Analysts.

Shah, S. M. I. 2009. Stratigraphy of Pakistan. Geological Survey of Pakistan. Memoirs, v.22.

Shah, S. M. I., Ahmed, R., Cheema, M. R., Fatmi, A. N., Iqbal, M. W. A., Raza, H. A., & Raza, S. M. (1997). Stratigraphy of Pakistan. Geological Survey of Pakistan. Memoirs, v. 12, p.137.

Shuaib, S. M. (1982). Geology and Hydrocarbon Potential of Offshore Indus Basin, Pakistan: Geologic Notes. AAPG bulletin, 66(7), 940-946.

Shuaib, S. M. (1982). Geology and Hydrocarbon Potential of Offshore Indus Basin, Pakistan: Geologic Notes. AAPG bulletin, 66(7), 940-946.

Shuaib, S. M., & Shuaib, S. T. (1994). Facies changes and hydrocarbon presence in offshore Indus Basin, Pakistan. Pakistan Journal of Hydrocarbon Research, 6(1 & 2), 2539.

Siddiqui, S. U. (1997, September). Hydrocarbon potential, offshore Pakistan. In 1st Annual Technical Convention of PAPG, Islamabad (pp. 26-27).

Silva, M. Da., Rauch-Davies, M., and Cuervo, A. 2004. Data conditioning for a combined inversion and AVO reservoir characterisation study, 66th EAGE Conf.

Simm, R., and Bacon, M. 2014. Seismic Amplitude: An interpreter's handbook, Cambridge University Press.

Stoneley, R. (1995). Introduction to petroleum exploration for no-geologists. Oxford University Press, USA.

Talwani, M., Worzel, J. L., & Landisman, M. (1959). Rapid gravity computations for two dimensional bodies with application to the Mendocino submarine fracture zone. Journal of geophysical research, 64(1), 49-59.

Tittman, J., & Wahl, J. S. (1965). The physical foundations of formation density logging (gamma-gamma). *Geophysics*, 30(2), 284-294.

Toqeer, M., Ali, A., Alves, T. M., Khan, A., & Hussain, M. (2021). Application of model based post-stack inversion in the characterization of reservoir sands containing porous, tight and mixed facies: A case study from the Central Indus Basin, Pakista. *Journal of Earth System Science*, 130(2), 1-21.

Vail, P. R., & Mitchum Jr, R. M. (1977). *Seismic Stratigraphy and Global Changes of Sea*

Vail, P. R., & Mitchum Jr, R. M. (1977). *Seismic Stratigraphy and Global Changes of Sea Level: Part 1. Overview: Section 2. Application of Seismic Reflection Configuration to Stratigraphic Interpretation.*

Vail, P.R., R.M. Mitchum, R.G. Todd, J.M. Widmer, S. Thompson, J.B. Sangree, J.N. Bubby and W.G. Hatfield (1977), *Seismic stratigraphy and global changes in sea level.* In: Payton (Ed.), *Seismic Stratigraphy: Application to Hydrocarbon Exploration*, AAPG-Memoir No. 26, AAPG, Tulsa, p. 49-212.

Vail, P.R., R.M. Mitchum, R.G. Todd, J.M. Widmer, S. Thompson, J.B. Sangree, J.N. Bubby and W.G. Hatfield,

Van Wagoner, J. C., Mitchum Jr, R. M., Posamentier, H. W., & Vail, P. R. (1987). *Seismic stratigraphy interpretation using sequence stratigraphy: Part 2: Key definitions of sequence stratigraphy.*

Veeken, P. C. (2006). *Seismic stratigraphy, basin analysis and reservoir characterisation (Vol. 37).* Elsevier.

Veeken, P. C. H. 2007. *Seismic Stratigraphy, Basin Analysis and Reservoir Characterisation*, Elsevier, Amsterdam.

Veeken, P. C. H., and Da Silva, M. 2004. *Seismic inversion methods and some of their constraints; First Break* 22 47–70.

Veeken, P. C. H., and Rauch-Davies, M. 2006. *AVO attribute analysis and seismic reservoir characterization; First Break* 24 41–52, <https://doi.org/10.3997/1365-2397.2006004>.

Walls, J., Dvorkin, J., and Carr, M. 2004. Well logs and rock physics in seismic reservoir characterization; Offshore Technol. Conf., <https://doi.org/10.4043/16921-MS>.

Wang, Y. 2017. Seismic Inversion: Theory and Applications, Wiley Blackwell.

White, R. 2003. Tying well-log synthetic seismograms to seismic data: The key factors; In: SEG Technical Program Expanded Abstracts 2003, Society Exploration Geophysicists, pp. 2449–2452, <https://doi.org/10.1190/1.1817885>.

Wyllie, M. R. J., Gregory, A. R., & Gardner, L. W. (1956). Elastic wave velocities in heterogenous and porous media. *Geophysics*, 21(1), 41-70.

Yao, F., and Gan, L. 2000. Application and restriction of seismic inversion; *Pet. Explor. Dev.* 27 53–56.

Yemets, V., Antoniuk, V., & Bezrodna, I. (2021). 21049 Facies interpretation from gamma ray (gr) log as basic well logs applied to Volodymyrska field (Dnipro-Donetsk depression). Online Event Geoinformatics.

Yilmaz, Ö. 2001. Seismic data analysis: Processing, inversion, and interpretation of seismic data, investigations in geophysics; Society of Exploration Geophysicists, <https://doi.org/10.1190/1.9781560801580>.